

AMERICAN UNIVERSITY OF BEIRUT

AEROSOL HEAT AND MASS TRANSFER IN THE
REGULATORY SCIENCE OF EMERGING TOBACCO
PRODUCTS

by
MARIO GEORGE EL HOURANI

A dissertation
submitted in partial fulfillment of the requirements
for the degree of Doctor of Philosophy
to the Department of Mechanical Engineering
of the Maroun Semaan Faculty of Engineering and Architecture
at the American University of Beirut

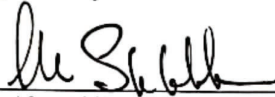


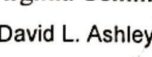

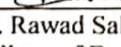
Beirut, Lebanon
April 2023

AMERICAN UNIVERSITY OF BEIRUT

AEROSOL HEAT AND MASS TRANSFER IN THE
REGULATORY SCIENCE OF EMERGING TOBACCO
PRODUCTS

by
MARIO GEORGE EL HOURANI

Approved by:

| | |
|--|----------------------------------|
|  Dr. Alan Shihadeh Department of Mechanical Engineering American University of Beirut | Signature Advisor |
|  Dr. Issam Lakkis Department of Mechanical Engineering American University of Beirut | Signature Chair of Committee |
|  Dr. Laleh Golshahi Department of Mechanical and Nuclear Engineering Virginia Commonwealth University | Signature Member of Committee |
|  David L. Ashley <small>Digitally signed by David L. Ashley Date: 2023.04.13 10:44:56 -04'00'</small> | Signature Member of Committee |
|  Dr. David Ashley Department of Population Health Sciences Georgia State University | Signature Member of Committee |
|  Dr. Rawad Saleh College of Engineering University of Georgia | Signature Member of Committee |

Date of dissertation defense: April 5, 2023

AMERICAN UNIVERSITY OF BEIRUT

DISSERTATION RELEASE FORM

Student Name: _____
El Hourani Mario George

I authorize the American University of Beirut, to: (a) reproduce hard or electronic copies of my dissertation; (b) include such copies in the archives and digital repositories of the University; and (c) make freely available such copies to third parties for research or educational purposes:

- As of the date of submission
- One year from the date of submission of my dissertation.
- Two years from the date of submission of my dissertation.
- Three years from the date of submission of my dissertation.

 _____ 04.26.2023
Signature Date

ACKNOWLEDGEMENTS

I would like to thank my advisors and committee members for their endless help, guidance, and motivation that was essential for the completion of this work. I would also like to acknowledge the help and support of all the aerosol lab members throughout my PhD studies. Finally, to my lovely wife Elyana and my family thank you for everything.

ABSTRACT OF THE DISSERTATION OF

Mario George El Hourani

for

Doctor of Philosophy

Major: Mechanical Engineering

Title: Aerosol Heat and Mass Transfer in The Regulatory Science of Emerging Tobacco Products

For decades, the tobacco industry has manipulated the sensory characteristics of tobacco products including the degree of harshness experienced at the back of the throat. Commonly referred to as “throat hit”, this harshness derives from absorption of gas-phase nicotine by the sensory nerves. Users learn to associate throat hit with the positive psychological effects of nicotine, making throat hit a secondary reinforcer for smoking. On the other hand, throat hit can make products aversive to nicotine naïve users and can mediate inhalation patterns. In recent years, ENDS manufacturers have increased nicotine content and lowered the freebase nicotine fraction of their products, making products that can deliver palatably a high nicotine dose. In this study we developed a simplified computational model of the heat and mass transfer processes for a nicotine-containing aerosol generated by an ENDS device of given power and liquid composition flowing through the mouth and throat. We compared computed nicotine absorption in the throat to reported subjective effects from previous clinical studies conducted by our group. Across various ENDS configurations, we found that computed nicotine absorption in the upper airways strongly predicted subjective harshness scores ($r=0.58$; $p<0.0001$). This finding indicates the technical feasibility of making ENDS throat hit a regulatory target, i.e. to reduce product appeal to prospective nicotine naïve users. In addition, this work comprises three additional studies directed at assessing toxicant origins, mouth level emissions, and nicotine emission rates of novel tobacco products.

TABLE OF CONTENTS

| | |
|--|-----------|
| ACKNOWLEDGEMENTS | 1 |
| ABSTRACT | 2 |
| ILLUSTRATIONS..... | 6 |
| TABLES..... | 7 |
| ABBREVIATIONS..... | 8 |
| | |
| PREDICTING “THROAT HIT” FROM ELECTRONIC NICOTINE DELIVERY SYSTEMS: A COMPUTATIONAL HEAT AND MASS TRANSFER MODEL OF NICOTINE ABSORPTION IN THE UPPER AIRWAYS | 10 |
| 1.1. Introduction..... | 10 |
| 1.2. Methods | 14 |
| 1.2.1. Overview..... | 14 |
| 1.2.2. Governing transport equations..... | 16 |
| 1.2.3. Airway geometry and discretization | 19 |
| 1.2.4. Airway wall heat and mass transfer coefficients | 20 |
| 1.2.5. Initial aerosol particle size at airway inlet | 22 |
| 1.2.6. Numerical solution..... | 23 |
| 1.2.7. Human subjective effects..... | 24 |
| 1.2.8. Statistical analysis..... | 25 |
| 1.3. Results and discussion | 25 |
| 1.3.1. Effect of device operating parameters on throat hit..... | 27 |
| 1.3.2. Throat nicotine vapor deposition and throat hit..... | 31 |
| 1.4. Conclusion | 32 |

DOES THE BUBBLER SCRUB KEY TOXICANTS FROM WATERPIPE TOBACCO SMOKE? MEASUREMENTS AND MODELING OF CO, NO, PAH, NICOTINE, AND PARTICULATE MATTER UPTAKE.....34

2.1. Introduction..... 34

2.2. Methods 35

 2.2.1. Study design..... 35

 2.2.2. Smoking machine protocol 36

 2.2.3. Sampling and analysis 36

 2.2.4. Statistical analysis..... 37

 2.2.5. Mathematical model description..... 37

 2.2.6. Mathematical model governing equations 38

 2.2.7. Numerical methods 39

2.3. Results..... 39

2.4. Discussion 41

2.5. Conclusion 43

COMPARISON OF CO, PAH, NICOTINE, AND ALDEHYDE EMISSIONS IN WATERPIPE TOBACCO SMOKE GENERATED USING ELECTRICAL AND CHARCOAL HEATING METHODS44

3.1. Introduction..... 44

3.2. Methods 46

 3.2.1. Experimental procedures 46

 3.2.2. EHE devices..... 46

 3.2.3. Optimal power determination 47

 3.2.4. Machine smoking and toxicant sampling protocol..... 48

 3.2.5. Statistical analysis..... 50

| | |
|--|-----------|
| 3.3. Results..... | 51 |
| 3.4. Discussion..... | 53 |
| 3.5. Conclusion | 54 |
| | |
| COMPARISON OF NICOTINE EMISSIONS RATE, “NICOTINE FLUX”, FROM HEATED, ELECTRONIC, AND COMBUSTIBLE TOBACCO PRODUCTS: DATA, TRENDS, AND RECOMMENDATIONS FOR REGULATION | 55 |
| 4.1. Introduction..... | 55 |
| 4.2. Methods | 58 |
| 4.3. Results..... | 59 |
| 4.4. Discussion..... | 64 |
| | |
| APPENDIX | 68 |
| | |
| REFERENCES | 74 |

ILLUSTRATIONS

Figure

| | |
|--|----|
| 1. Figure 1: Schematic representation of the modeled system consisting of the ENDS device and upper airway..... | 15 |
| 2. Figure 2: Upper airway geometry and sections | 20 |
| 3. Figure 3: Temperature variation along the upper airway at 5 and 10 SLPM obtained from the CFD simulations and the developed mathematical model. The inlet aerosol temperature was 373K while the airway wall temperature was constant at 310K. | 22 |
| 4. Figure 4: Aerosol component concentration variation along the airway for condition A. | 29 |
| 5. Figure 5: Aerosol temperature and particle phase molar fractions variation along the airway for condition A. | 29 |
| 6. Figure 6: Predicted segmental nicotine vapor deposition rates per cm ² of throat surface area at conditions shown in table 4. | 31 |
| 7. Figure 7: Subjective throat hit sensation vs model predicted throat hit..... | 32 |
| 8. Figure 8: Subjective throat hit sensation vs model predicted nicotine flux for all conditions of studies of (S1) and (S2) – N=233 | 32 |
| 9. Figure 9: Schematic of a waterpipe a) unmodified, and b) configured such that the smoke bypasses the water bubbler. | 35 |
| 10. Figure 10: Simulation results showing evolution of component mass relative to initial mass for a hypothetical aerosol consisting of water, glycerin, nicotine, and benzo(a)pyrene trapped in a 1 cm bubble rising through a 3 cm column of water at 25 °C. Initial aerosol conditions: 3.5x10 ⁶ particles/m ³ , particle diameter: 100 nm. | 42 |
| 11. Figure 11: Relationship between liquid nicotine concentration, device power, flux (nicotine emission rate), and yield for an ENDS device by analogy to a reservoir emptying into a container through a valve and tap assembly. In this analogy, the electrical power of the ENDS device determines the degree to which the tap is open during a puff; greater power means a more open valve... | 57 |
| 12. Figure 12: Reported nicotine flux of ENDS products by year of manuscript publication. (p<0.001 for both regression lines)..... | 64 |
| 13. Figure 13: Nicotine flux ranges across tobacco products. The dashed line for ENDS represents the capacity of current over-the-counter products to exceed values reported to date. | 66 |

TABLES

Table

| | |
|--|----|
| 1. Table 1: Activity coefficient of nicotine in solution for various PG/VG ratios . | 18 |
| 2. Table 2: Conditions of studies (S1) and (S2) differing by the power of the sub-ohm device used (SUBOX Mini-C), nicotine concentration and form. The PG/VG ratio of all conditions was 30/70..... | 25 |
| 3. Table 3: Predicted nicotine vapor deposition in the upper airway during a 4 second puff for five conditions that differ by power (15 vs 30 W), nicotine concentration (5 vs 10 mg/ml), freebase fraction (10 vs 90 %), and inhalation flow rate (5 vs 10 slpm). | 27 |
| 4. Table 4: The initial input parameters used in the model. x represents the initial mass fractions of the individual components. dp and dB are the particle and bubble diameters, respectively. N_0 is the initial number concentration of particles inside the bubble..... | 39 |
| 5. Table 5: Toxicant yields [mean (standard deviation)] for N=5 repeated sessions for each condition. * indicates statistically significant difference relative to baseline condition. ND indicates below instrument detection limits..... | 40 |
| 6. Table 6: Schematic representation of the EHEs used in this study, in addition to their material properties and operation range. | 47 |
| 7. Table 7: Thermal performance, CO, Nicotine, PAHs and CCs yields [mean (standard deviation)] for N=3 smoking sessions according to the reduced Beirut smoking protocol. | 53 |
| 8. Table 8: Summary of the nicotine yield and flux of various tobacco products and the corresponding puffing topography parameters. * Average puff number under ISO smoking regime was used..... | 63 |
| 9. Table 9: Computed nicotine flux by tobacco product category. N indicates the number of products reported, while year span indicates years of publication for the studies included. SD = standard deviation. | 63 |
| 10. Table A1: Nusselt number values in the oral cavity “OC” at flow rates ranging between 1 and 20 liters/minute | 72 |
| 11. Table A2: Nusselt number values in the laryngeal tracheal airway “LT” at flow rates ranging between 1 and 20 liters/minute | 73 |

ABBREVIATIONS

A_s : Surface area (m^2)
 c_p : Specific heat ($J/kg.K$)
CN: Coupling number
 d : diameter (m)
 d_{hyd} : Hydraulic diameter (m)
 $\frac{dm_{p,i}}{dt}$: Mass change of aerosol component in the particle phase (kg/s)
 D_v : Vapor diffusion coefficient in air (m^2/s)
 h : Heat transfer coefficient (W/m^2K)
 h_m : Mass transfer coefficient (m/s)
 \bar{h} : Average heat transfer coefficient (W/m^2K)
 k : Thermal conductivity (W/mK)
 K : Kelvin ratio
 L : Length (m)
 L_e : Lewis number
 m : Mass (kg)
 \dot{m} : Mass flow rate (kg/s)
 \dot{m}_{v_0} : Aerosol vaporization rate (kg/s)
 M : Molar mass (kg/mol)
 n_f : Molar fraction in the particle phase
 N_p : Particle number concentration (particles/ m^3)
 N_u : Nusselt number
 P_b : Bulk pressure (Pa)
 P_{er} : Perimeter (m)
 P_s : Saturation pressure (Pa)
 \dot{Q} : Heat transfer rate (W)
 \dot{Q}_p : Heat transfer by conduction from a single particle to the surrounding bulk (W)
 \dot{Q}'_w : Convective heat transfer from bulk to airway wall per unit volume (W/m^3)
 R : Universal gas constant ($\frac{J}{K.mol}$)
 Re_D : Reynolds number
 T : Temperature (K)
 T_m : Mean temperature (K)
 V : Volume (m^3)

Greek letters

γ : Surface tension (N/m)
 ρ : Density (kg/m^3)
 α_{fb} : Free base nicotine mass fraction
 ΔC : Concentration gradient between aerosol bulk and airway walls (kg/m^3)
 Φ : Fuchs correction factor
 ζ : Activity coefficient in the mixture

Subscripts

a : Air
 w : Airway wall

b: Bulk
fb: free-base nicotine
i: Aerosol component index
nic: nicotine
p: particle
v: vapor

CHAPTER 1

PREDICTING “THROAT HIT” FROM ELECTRONIC NICOTINE DELIVERY SYSTEMS: A COMPUTATIONAL HEAT AND MASS TRANSFER MODEL OF NICOTINE ABSORPTION IN THE UPPER AIRWAYS

1.1. Introduction

The World Health Organization estimates that tobacco use kills 8 million people every year, and is a leading preventable cause of death and disease¹. Containing the addictive psychomotor stimulant nicotine, tobacco smoke is a highly concentrated aerosol made of liquid particle droplets and gas molecules². For cigarettes, the inhaled mainstream aerosol contains more than 7000 chemical compounds, 150 of which are thought to be toxic³. These toxic compounds can induce various adverse health effects including pulmonary inflammation, lung cancer, chronic obstructive pulmonary disease (COPD), cardiovascular disease, reproductive and developmental effects, and the suppression of the immune system⁴.

In recent years electronic nicotine delivery systems (ENDS) became prevalent⁵. ENDS are battery-operated devices that vaporize a liquid mixture and deliver nicotine to users via an inhalable aerosol^{6,7}. Various liquid compositions and flavors are commercially available and can also be custom made by users⁸. While ENDS liquids vary in composition, they usually contain vegetable glycerin (VG), propylene glycol (PG), nicotine, and flavorants^{6,7} that appeal to youth and adults⁹. ENDS contain an electrical heating coil that contacts a wick which draws liquid from a reservoir. When a user draws a puff, the coil is activated and the nicotine-containing liquid is heated and

vaporized from the wick, producing a dense, visible aerosol⁷. The heating process also leads to formation of toxicants that were not originally in the liquid¹⁰⁻¹². Various compounds including nicotine are released into the gas phase at the hot coil/wick interface. As the vapors are convected away from the heated interface by the action of puffing, the semi-volatile components, including nicotine, condense and partition between particle and gas phases in the aerosol.

While most tobacco users have attempted to quit¹³, consumption remains prevalent due to the addictive nature of tobacco products. The psychomotor stimulant nicotine is the main addictive agent in tobacco aerosols and it is widely thought that without it tobacco consumption would not be sustained^{14,15}. The inhaled aerosol delivers nicotine to the brain within seconds following its absorption in deep airways and subsequent distribution through the cardiovascular system¹⁶. Nicotine reaches the mesolimbic reward pathway of the brain and attaches to nicotinic receptors on neurons, activating the release of dopamine, a neurotransmitter that leads to a sense of pleasure and reward¹⁶. The centrality of nicotine delivery to continued smoking led the tobacco industry to design products that efficiently deliver nicotine to the brain by optimizing both nicotine emissions and sensory characteristics of the inhaled aerosol. These factors largely govern the dose of inhaled nicotine by the user¹⁷. The rate of nicotine emission per puff second from a given tobacco product (i.e. “nicotine flux”¹⁸) depends on product design parameters (e.g. nicotine content, filter design, length and diameter for combustible cigarettes, and device power, and liquid nicotine concentration for ENDS).

On the other hand, sensory characteristics of the inhaled aerosol can influence user puff topography and inhalation patterns. For example, cigar smoke is too harsh to

be inhaled deeply and therefore results in slower delivery of nicotine to the brain than a cigarette because nicotine uptake through the tissues of the oral cavity is far slower than the distribution of nicotine into the blood stream across the alveoli in the lung¹⁹.

Sensory characteristics can be manipulated by using additives such as menthol to increase palatability²⁰, and pyrazine to amplify tobacco flavor and modulate upper airway harshness²¹. Another important mechanism for manipulating sensory characteristic involves altering nicotine form. Nicotine can exist in two forms in the aerosol of tobacco products: free base (Nic) and protonated (Nic-H⁺). Protonated nicotine is acidic and non-volatile and can be present only in the particle phase. On the other hand, free base nicotine partitions between the particle and vapor phases to attain phase equilibrium². All else held constant, the vapor phase nicotine concentration in a tobacco aerosol varies with the product of the nicotine mole fraction in the particle phase, the fraction of the nicotine in the free-base form, and the thermodynamic vapor pressure of freebase nicotine at the aerosol temperature (i.e. increasing aerosol temperature will also increase vapor phase nicotine concentration).

Nicotine vapor is absorbed efficiently in the oral cavity and upper airways during inhalation, and results in a harsh sensory “impact” known as “throat hit”, “throat grab”, or “throat scratch”. The harsh sensation is thought to derive from absorption of nicotine vapor in the region of the sensory nerves at the back of the throat²².

Internal tobacco industry documents²³⁻²⁵ indicate that for decades the industry has been aware of the role of nicotine vapor in generating throat hit, and extensively studied the matter empirically. For example, a 1991 internal report²³ by R.J. Reynolds cited various company studies of the processes of nicotine deposition in the throat and related subjective effects in human participants. Among the studies reported was one in

which smokers found that cigarettes with acids added to the tobacco during manufacturing elicited less throat hit than even low nicotine content cigarettes which had not been processed with an acid. Adding acid to tobacco converts free-base to protonated nicotine, and reduces the equilibrium concentration of vapor phase nicotine when that tobacco is smoked²⁶. It is clear from the internal industry documents that tobacco companies believed that gas-phase nicotine concentration is the main determinant of throat hit sensation and is a function of nicotine concentration in aerosol particles as well as its form (protonated versus freebase).

While throat hit might play a major role in the appeal/aversiveness balance of a certain tobacco product, it may also affect user puffing patterns (i.e. puff topography: duration, volume, interpuff interval). In particular, greater throat hit may result in shorter and fewer puffs due to irritation, and potentially impact nicotine delivery and abuse liability, including use of ENDS by previously naïve youth. If so, throat hit may be an attractive and potentially powerful regulatory target for public health ends.

In this work, we sought to develop a computational model that could be used to predict throat hit of ENDS products, and its sensitivity to factors such as liquid composition, device characteristics and inhalation patterns. We hypothesized that a simplified 1-D Lagrangian model of an aerosol flowing through an idealized mouth-throat model would capture patterns in reported throat hit from participants in clinical studies who used various ENDS products.

1.2. Methods

1.2.1. Overview

The problem at hand is to compute nicotine vapor absorption in the sensory nerves region of the throat as a user inhales from an ENDS product with known geometry, electrical power, and liquid composition with given PG, VG, nicotine concentrations, and freebase/protonated nicotine ratio. The approach taken involves following a bolus of aerosol emitted by the ENDS as it travels through the mouth and throat. During a puff, the aerosol is assumed to be inhaled directly from the device into the mouth and lung in a one-step process that ENDS users term “direct-to-lung”. During each puff, the flow was assumed steady and one dimensional in the axial direction of the airway at each discrete flow segment. We found that for a given aerosol mass concentration and composition, nicotine absorption in the upper airways was insensitive to particle diameter over the size ranges previously reported in the literature⁷ and we therefore modeled the aerosol as monodisperse and neglected coagulation.

Initially in phase equilibrium, when the relatively warm aerosol bolus enters the mouth it is subject to a flow boundary whose temperature and humidity are 37.5 C and 100% relative humidity, respectively. The difference in temperature and humidity between the walls and the aerosol creates thermal and mass concentration gradients that drive continuous transport of species and thermal energy between the walls, the bulk, and the particle phase. Broadly, the aerosol gains moisture and cools as it passes through the mouth and throat, while simultaneously the walls absorb thermal energy and volatile species from the aerosol, namely freebase nicotine, PG, and VG.

The composite system model in this study therefore consists of the ENDS device and the mouth-throat, as shown in Figure 1. The ENDS model used in this work is

detailed in Talih et al. (2017), and takes as inputs the device power, liquid composition, device geometry and user puff topography and computes the time-resolved temperature and the mass concentration and composition of the multicomponent aerosol that exits the heating coil/wick assembly of the ENDS. To compute the temperature of the aerosol exiting the ENDS mouthpiece, we coupled the ENDS model of Talih et al. (2017) to a boundary-layer heat transfer model using the geometry of the Subox Mini-C ENDS product used in the clinical studies (described below) to determine the aerosol temperature at the exit of the device mouthpiece. The exit temperature was verified by measurements described in the Appendix. The temperature, mass concentration, and composition at the mouthpiece exit are then taken as the inlet conditions for the mouth-throat computations.

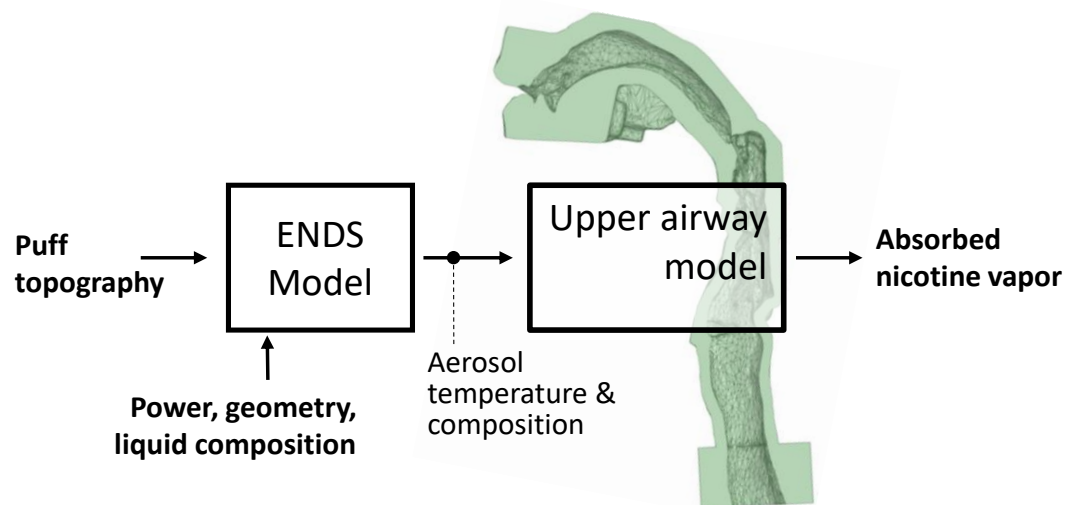


Figure 1: Schematic representation of the modeled system consisting of the ENDS device and upper airway.

The modeled airway domain extends from the mouth to the upper trachea, and the flow in it is treated as one-dimensional. The domain is discretized along the axial direction, and at each airway segment the temperature and composition of the aerosol is computed using energy and species balances. The heat and mass exchange between the

bulk phase of the aerosol and moist airway walls, as well as between the aerosol particles and the bulk phase are computed at each segment. ENDS aerosol particles are small enough to be treated as quiescent with respect to the surrounding vapors, and the heat and mass transfer between the vapor and particle phases is sufficiently small that it can be computed using Maxwell's quasi-stationary diffusion equation²⁷. The total nicotine absorbed during a puff is computed at each location by summing the nicotine absorbed at each time step of the simulation. Particle deposition in the upper airways is negligible due to the low Stokes number and low diffusion coefficient of particles in the 50-500 nm size range which is typical of ENDS aerosols²⁸.

Energy and mass exchanges between the bulk and airway wall are computed at each segment using a boundary layer formulation in which the local heat transfer coefficient is determined by fitting to a 3D computational fluid dynamics simulation described below. Mass transfer coefficients were determined from the heat transfer coefficient using the heat-mass transfer analogy²⁹.

Finally, the utility of the model was demonstrated by comparing computed rates of nicotine vapor absorption in the throat region to reported scores of subjective "throat hit" sensation from recently conducted clinical studies with varying ENDS products. Each of these aspects of the work is described below in more detail.

1.2.2. Governing transport equations

As the aerosol flows into the upper airways, gas-phase mass transfer to/from the airway walls is initiated by concentration and temperature differences between the relatively warm and dry aerosol bulk phase and the relatively cool water-saturated airway walls. This exchange of mass and heat between the walls and the bulk results in

a dynamical system in which particles continuously absorb water vapor and lose thermal energy as they flow downstream. The rate of vapor mass transfer to/from the particle surfaces is a function of the particle composition, size, and vapor pressure of individual aerosol species, which, in turn, changes with particle temperature. The relevant variables are related through the mass, species, and energy conservation equations, and thermodynamic properties of the various species, as given below, for a monodisperse aerosol system flowing through a given airway segment.

Vapor mass transfer rate to/from airway walls:

$$\dot{m}_{v,i} = h_{m,i} A_s \Delta C_i \quad (1)$$

Where the subscript “*i*” refers to individual species (i.e. nicotine, PG, VG, and water), and $h_{m,i}$ is the mass transfer coefficient for the correspondent species.

Bulk phase species conservation:

$$\frac{dC_i}{dt} = N_p \frac{dm_{p,i}}{dt} - \frac{\dot{m}_{v,i}}{V} \quad (2)$$

Where N_p is particle number concentration, $m_{p,i}$ is the mass of species *i* in the particle phase, and V is the volume of the airway segment.

Particle phase evaporation/condensation:

$$\frac{dm_{p,i}}{dt} = 2\pi\Phi d_p D_{v,i} \frac{M_i}{R} \left(\frac{P_{b,i}}{T_b} - \frac{P_{s,i}}{T_p} \right) \quad (3)$$

The rate of change of the mass of species *i* in the particle $\frac{dm_{p,i}}{dt}$ is corrected for non-continuum effects via the Fuchs correction factor, $\Phi = \frac{2\lambda + d_p}{d_p + 5.33(\lambda^2 d_p) + 3.42\lambda}$. The vapor pressure of species *i* at the particle surface, $P_{s,i}$, was computed as the product of the mole fraction and the thermodynamic saturation pressure of that component evaluated

at the droplet temperature, modified by the activity coefficient ζ_i to account for non-ideal solution behavior, and the Kelvin effect multiplier K to account for pressure elevation due to droplet surface curvature in a liquid with surface tension γ_p :

$$P_{s,i} = \zeta_i K n_{f,i} P_{v,i} \quad (4)$$

$$K = \left(\frac{4\gamma_p M_p}{\rho_p R T_p d_p} \right) \quad (5)$$

For nicotine transport, equation (4) is also multiplied by the free-base fraction of nicotine in particle phase α_{fb} . While ζ for PG and VG is near unity, semi-polar molecules such as nicotine exhibit an activity coefficient greater than unity³⁰. Pankow et al.³⁰ determined an activity coefficient of 2.1 for nicotine in a 50/50 PG/VG solution. We used the COSMO-RS tool from the Amsterdam Density Functional software package (Software for Chemistry and Materials³¹) to determine ζ at other PG/VG ratios (shown in Table 1).

| <i>PG/VG</i> | <i>Nicotine activity coefficient</i> |
|--------------|--------------------------------------|
| 100/0 | 1.16 |
| 70/30 | 1.67 |
| 50/50 | 2.25 |
| 30/70 | 3.17 |
| 0/100 | 5.82 |

Table 1: Activity coefficient of nicotine in solution for various PG/VG ratios

Particle temperature:

$$m_p c_{p,p} \frac{dT_p}{dt} = \dot{Q}_p \quad (6)$$

Where $\dot{Q}_p = 2\pi k_a d_p (T_b - T_p)$ is the heat transfer rate by conduction from a single droplet to the bulk phase.

Bulk phase temperature:

$$\rho_a c_{p,a} \frac{dT_{m,b}}{dt} = -N_p \dot{Q}_p + \dot{Q}'_w \quad (7)$$

Where $\dot{Q}'_w = \frac{hA_s}{V}(T_b - T_w)$ is the heat transfer rate by convection per unit volume from the aerosol bulk to the airway walls. Air properties are used for the bulk phase because the mass concentration of all other species combined is orders of magnitude less than air.

1.2.3. Airway geometry and discretization

The mouth-throat model used in this study was derived from a computed tomography scan of an adult volunteer and is described in detail in Golshahi et. al (2023). The geometry shown in Figure 2 comprises the oral cavity (OC) and the laryngeal tracheal (LT) airway. The OC extends from the oral entrance to the oropharynx (the starting point of the pharynx), while the LT airway stretches from the oropharynx to the upper trachea. The geometry was dissected into 67 sections also shown in Figure 2, so that the perimeter and cross-sectional area of each section could be determined. All sections were chosen to be normal to the local axis of the airway. It is assumed that the perimeter and cross-sectional area of the airway segment between two consecutive sections are constant and equal to the average of the two sections. The hydraulic diameter at any airway segment can be computed as:

$$d_{hyd} = 4 \frac{V_{aw}}{A_{s,aw}} \quad (8)$$

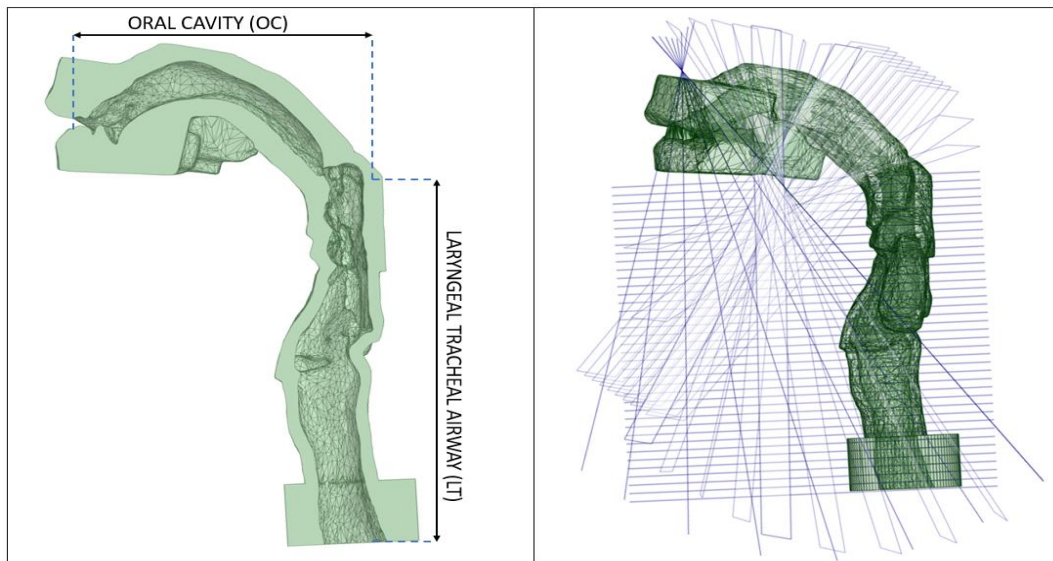


Figure 2: Upper airway geometry and sections

The total length of the OC was 7.3 cm, with an average perimeter and cross-sectional area of 6.52 cm and 1.62 cm², respectively. The LT airway was 11.4 cm in length, with the perimeters and cross-sectional areas averaging at 6.00 cm and 1.79 cm² respectively. The cross-sectional areas, perimeters, and hydraulic diameters of the OC and LT airway are provided in the Appendix.

1.2.4. Airway wall heat and mass transfer coefficients

To determine the relevant values of the local mean heat and mass transfer coefficients along the airway, flow through the detailed upper airway geometry was simulated in 3-D using the ANSYS FLUENT software package. Simulated flow rates ranged from 1 to 20 SLPM, in 1 SLPM increments. The Mesh tool in ANSYS was used to geometrically discretize the upper airway in approximately five million regular tetrahedral-shaped elements ranging in size between 0.12 and 0.74 mm at an average edge size of 0.38 mm. A laminar viscous model was employed for flow rates between 1 and 4 l/min, and a transition SST k-omega model was employed at the remaining flow

rates. The inlet flow temperature was set to 373 K, while the airway walls were set to 310 K. The mean air temperature was computed at each of the 67 sections of the discretized model. Based on the temperature change across each flow segment, the local heat transfer coefficient could be determined. Nusselt number values were then calculated at each airway section for each flow rate as

$$N_u = \frac{hd_{hyd}}{k_a} \quad (9)$$

A lookup table was generated for Nusselt number values at each airway section and flow rate (see Appendix). To verify the approach, temperature predictions using the 1-D flow formulation and lookup table were compared to those obtained from the 3-D ANSYS simulations. Figure 3 shows the obtained cross-sectional mass-weighted mean temperature along the airway at two representative flow rates, 5 and 10 l/min, for the 3-D CFD simulations and simplified 1-D model. As shown, the computed temperatures were in good agreement. Simulations were also run at an inhalation temperature of 323K and the resulting temperature profiles also showed very good agreement (results not shown). The mass transfer coefficient of any component in the aerosol can be obtained from heat and mass transfer analogy²⁹ by:

$$h_{m,i} = \frac{D_{v,i} h L e^{\frac{1}{3}}}{k_a} \quad (10)$$

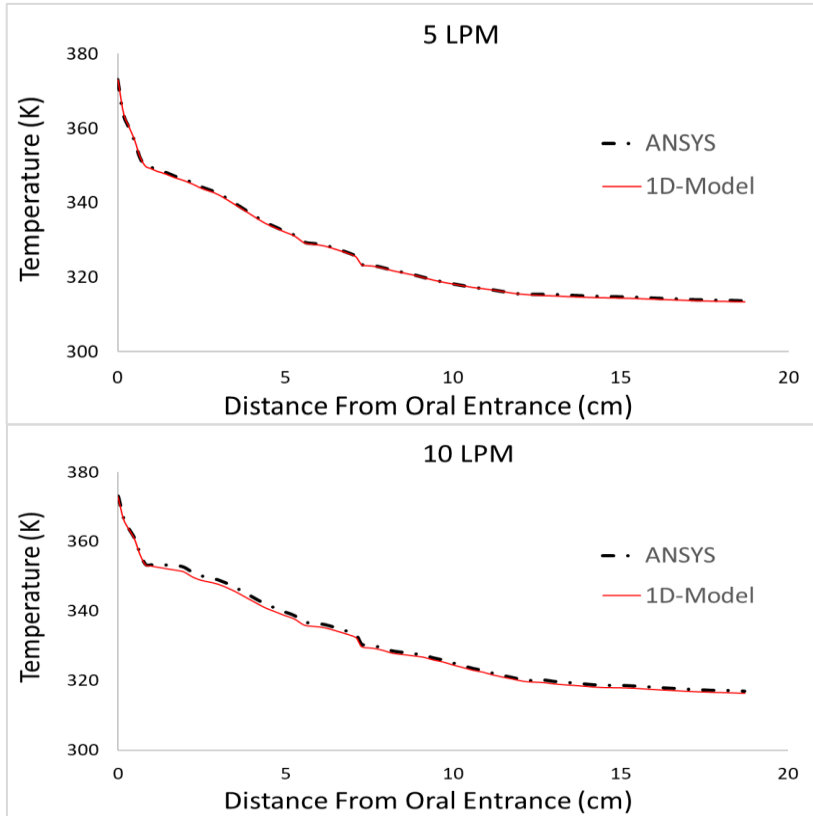


Figure 3: Temperature variation along the upper airway at 5 and 10 SLPM obtained from the CFD simulations and the developed mathematical model. The inlet aerosol temperature was 373K while the airway wall temperature was constant at 310K.

1.2.5. Initial aerosol particle size at airway inlet

The condensation sink diameter corresponding to a typical particle size distribution of the aerosol of ENDS was used⁷. As described by Lehtinen et al.³², the condensation sink diameter is the particle diameter of a monodisperse aerosol exhibiting the same net condensation or evaporation rate as a polydisperse aerosol. For the ENDS particle size distributions measured by Baasiri et al.⁷, calculated condensation sink diameters were 152 nm, 130 nm, and 64 nm for PG/VG ratios of 0/100, 70/30, and 100/0 respectively. However, in the current study simulations showed that the rate of nicotine vapor absorption in the throat region did not vary significantly across a wide range size range of ENDS aerosols. The independence from particle size can be viewed

through the coupling number, which is defined for an aerosol flowing through a tube as the ratio of the rate at which vapors condense/evaporate from the particle phase to the rate at which vapors condense/evaporate from the tube walls³³:

$$CN = \frac{2\pi d_p(\rho_a C_{pa} \alpha) d_{hyd}}{h} \quad (11)$$

Owing to the high number concentrations, the coupling number for ENDS aerosols is several orders of magnitude greater than unity, which means that the particle phase adjusts instantly to boundary heat/mass transfer induced changes in the vapor phase, even across a tenfold change in aerosol particle diameter. Therefore, to simplify presentation of results, all simulations reported below assume a particle diameter of 100 nm, with a mass concentration, aerosol composition, and temperature computed by the ENDS model for the conditions examined.

1.2.6. Numerical solution

A Lagrangian approach was implemented to model the aerosol flow in the upper airway, wherein a differential volume of aerosol with moving control surfaces was tracked in time. The differential volume equals the local volumetric flow rate multiplied by the time step dt and geometrically takes the shape of the airway walls. At each time step, the tracked aerosol volume moves by its width dl such that $dl = v_n dt$ where v_n is the average axial velocity, resulting in a Courant Number of unity. Airway surface area, hydraulic diameter, and Nusselt number values were obtained at each time step from lookup tables depending on the location of the tracked volume in the upper airway.

At each time step, the heat and mass transfer differential equations were solved simultaneously in the MATLAB computing environment using a first order explicit

finite difference scheme. A time step of 1×10^{-7} s was found to be sufficiently small to assure time-step independent results.

1.2.7. Human subjective effects

We retrieved data from two recent clinical studies performed by our group at the Virginia Commonwealth University (VCU) in which subjective throat hit was reported following electronic cigarette use. These studies involved ENDS liquid compositions with varying freebase fraction, nicotine concentration, and electrical power. In the first study (S1)³⁴, 32 participants used a sub-ohm electronic cigarette (SUBOX Mini-C) under four conditions differing by device power, liquid nicotine concentration and form as shown in Table 2. For all conditions of study S1 nicotine was predominantly in the free-base form. For each of the four conditions, participants used the ENDS device for a 10-puff directed bout followed by a 60-minute ad-lib smoking period.

In the second study (S2)³⁵, 23 ENDS users were recruited and underwent a similar smoking sequence as in study (S1), but this time nicotine was mostly in the protonated form. Table 2 also summarizes the conditions of study (S2).

| Condition | <i>Nicotine Concentration (mg/ml)</i> | <i>Freebase Nicotine Mass %</i> | <i>Device Power (W)</i> |
|-----------|---------------------------------------|---------------------------------|-------------------------|
| S1-1 | 8 | 83 | 40.5 |
| S1-2 | 3 | 83 | 40.5 |
| S1-3 | 8 | 93 | 13.5 |
| S1-4 | 3 | 93 | 13.5 |
| S2-1 | 10 | < 1 | 15 |
| S2-2 | 15 | < 1 | 15 |
| S2-3 | 30 | < 1 | 15 |
| S2-4 | 10 | < 1 | 30 |
| S2-5 | 15 | < 1 | 30 |
| S2-6 | 30 | < 1 | 30 |

Table 2: Conditions of studies (S1) and (S2) differing by the power of the sub-ohm device used (SUBOX Mini-C), nicotine concentration and form. The PG/VG ratio of all conditions was 30/70.

Outcomes of both studies included puff topography (i.e. number of puffs, puff duration, interpuff interval, and flow rate) and various subjective effects including throat hit sensation. Throat hit sensation was reported on an analog scale ranging from 0 (minimum) to 100 (maximum). For both studies the ten-puff directed bout was used for correlation against model predictions of nicotine throat deposition. Model simulations were run for each participant using average values of the measured puff topography parameters corresponding to each use condition, resulting in a total of N=127 and N=106 conditions for studies (S1) and (S2) respectively.

1.2.8. Statistical analysis

Linear regression of predicted and measured variables was performed using SPSS version 23.0 (IBM, Armonk, NY, USA). Statistical significance was set at $p < 0.05$.

1.3. Results and discussion

Across all conditions, the simulations showed that when the ENDS aerosol enters the oral cavity, most of the nicotine (circa 90%) is found in the particle phase. Near the entrance of the oral cavity, PG, VG, and nicotine vapors are scavenged by the relatively cool walls, causing evaporation from the particle phase to restore phase equilibrium. As the aerosol flows further into the cavity it loses heat to walls, resulting in a drop in temperature and therefore vapor pressure of its components. This drop reduces the equilibrium vapor mass concentration of all the semi-volatile species, including nicotine. The drop in temperature also accelerates water vapor uptake from

the oral cavity to the particles, which, in turn, dilutes the particle phase nicotine concentration and further lowers the equilibrium nicotine vapor concentration. As a result of these overlapping processes, by the time the aerosol enters the throat, the particle phase nicotine has been diluted by water by nearly 50% and the mass concentration of vapor phase nicotine has been reduced by 80%. Thus the simulations indicate that the oral cavity plays a major role in humidifying and cooling the aerosol and denudes it of most of the nicotine vapor prior to its entry into throat. Even without mouth-hold, the oral cavity greatly modulates throat hit.

Another salient feature of the nicotine absorption dynamics observed across all conditions was that the condensed phase provides almost none of the nicotine that causes throat hit. Contrary to the intuitive notion that the particles represent a large nicotine reservoir that continuously feeds the vapor phase to make up for that absorbed by the flow boundaries, the particle phase competes with the oral cavity and throat walls for vapor phase nicotine. In other words, the simulations showed that throat deposition of nicotine would actually increase if the particle phase had been trapped by a filter prior to entering the oral cavity.

Thus, to a first approximation, the simulations indicate that the initial vapor phase nicotine is the dominant factor governing throat hit. With regard to segmental deposition of nicotine in the throat, we found that the first third of the laryngeal tracheal airway had the greatest deposition flux, due to the combination of the relatively elevated vapor nicotine concentration and high convection coefficient. Finally, the simulations showed that inhalation velocity has a significant effect on throat absorption, with greater velocities resulting in a greater absorption of nicotine at the walls due to

enhanced convective mass transfer rates. These and other effects are examined in more detail below.

1.3.1. Effect of device operating parameters on throat hit

The effect of device operating parameters and user smoking behavior on nicotine vapor deposition in the upper airway was tested by running the model at five conditions summarized in table 3, where device power, nicotine concentration, freebase nicotine fraction and flow rate were varied individually with respect to reference condition A. For all simulated conditions, the PG/VG ratio was 30/70. Table 3 also presents the predicted total mass of nicotine inhaled in addition to the total nicotine vapor mass deposited during a four second puff in both the oral cavity and laryngeal tracheal airway.

| Condition | Device Power (W) | Nicotine Concentration (mg/ml) | Freebase Nicotine Mass (%) | Flow Rate (l/min) | Total Nic. Inhaled (µg) | Nic. Vapor Inhaled (µg) | Nic. Vapor Deposition in OC (µg) | Nic. Vapor Deposition in LT (µg) |
|------------------|-------------------------|---------------------------------------|-----------------------------------|--------------------------|--------------------------------|--------------------------------|---|---|
| A | 30 | 10 | 90 | 10 | 473 | 47 | 11 | 2.6 |
| B | 15 | 10 | 90 | 10 | 124 | 8.1 | 2.6 | 1 |
| C | 30 | 5 | 90 | 10 | 235 | 23 | 5.5 | 1.3 |
| D | 30 | 10 | 90 | 5 | 385 | 42 | 10 | 1.6 |
| E | 30 | 10 | 10 | 10 | 431 | 5.2 | 1.2 | 0.3 |

Table 3: Predicted nicotine vapor deposition in the upper airway during a 4 second puff for five conditions that differ by power (15 vs 30 W), nicotine concentration (5 vs 10 mg/ml), freebase fraction (10 vs 90 %), and inhalation flow rate (5 vs 10 slpm).

Simulation results show that the predominant nicotine vapor deposition in the upper airways takes place in the oral cavity and ranges between 60 to 85% of the total nicotine vapor deposition across the five simulated conditions. This can be attributed to the higher mass transfer coefficients in the oral cavity compared to the LT airway and to higher nicotine vapor concentration gradients between the aerosol bulk and airway walls in the oral cavity. Moreover, the aerosol loses heat to the airway walls as it flows

in the upper airway resulting in the decrease of the vapor pressure of individual aerosol components including nicotine. In addition, the bulk water vapor concentration increases along the flow direction and results in the dilution of the particle due to water vapor condensation and a drop in the molar fraction of nicotine, PG, and VG. This will lead to a lower resistance to nicotine vapor condensation to the particle phase as a result of equation (3) and less nicotine vapor will be available in the aerosol bulk for mass transfer to the airway walls. These processes are illustrated in figures 4 and 5 showing the evolution of bulk phase concentrations of aerosol components, aerosol bulk temperature, and particle phase molar fractions along the airway for condition A.

A second observation from Table 3 is that there is no clear correlation between throat nicotine vapor deposition and the total mass of inhaled nicotine. The total mass of inhaled nicotine for condition E is similar to condition A and several times higher than conditions B to D yet nicotine vapor throat deposition of condition E is significantly lower than the other four conditions. The effect of nicotine flux on throat deposition is further discussed in the next section.

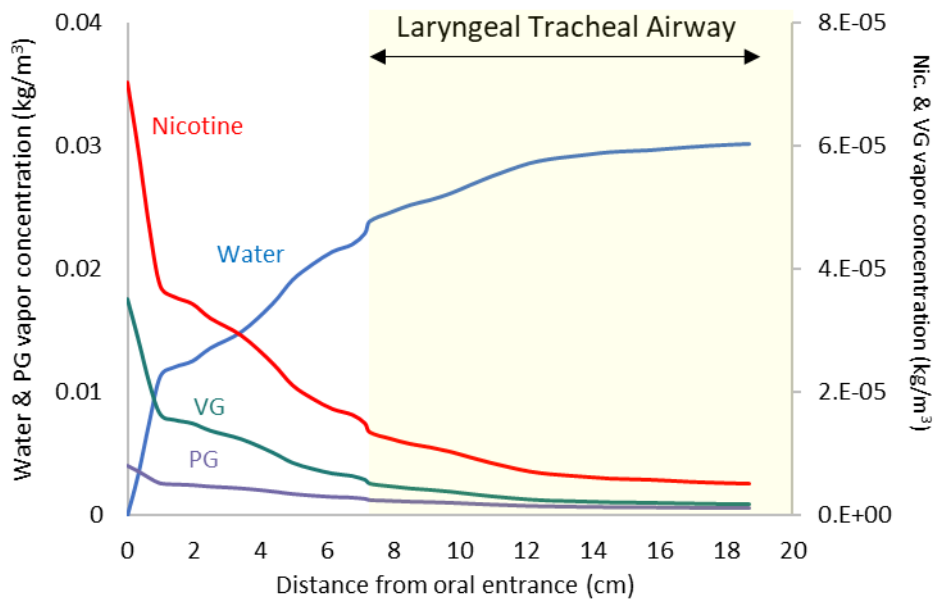


Figure 4: Aerosol component concentration variation along the airway for condition A.

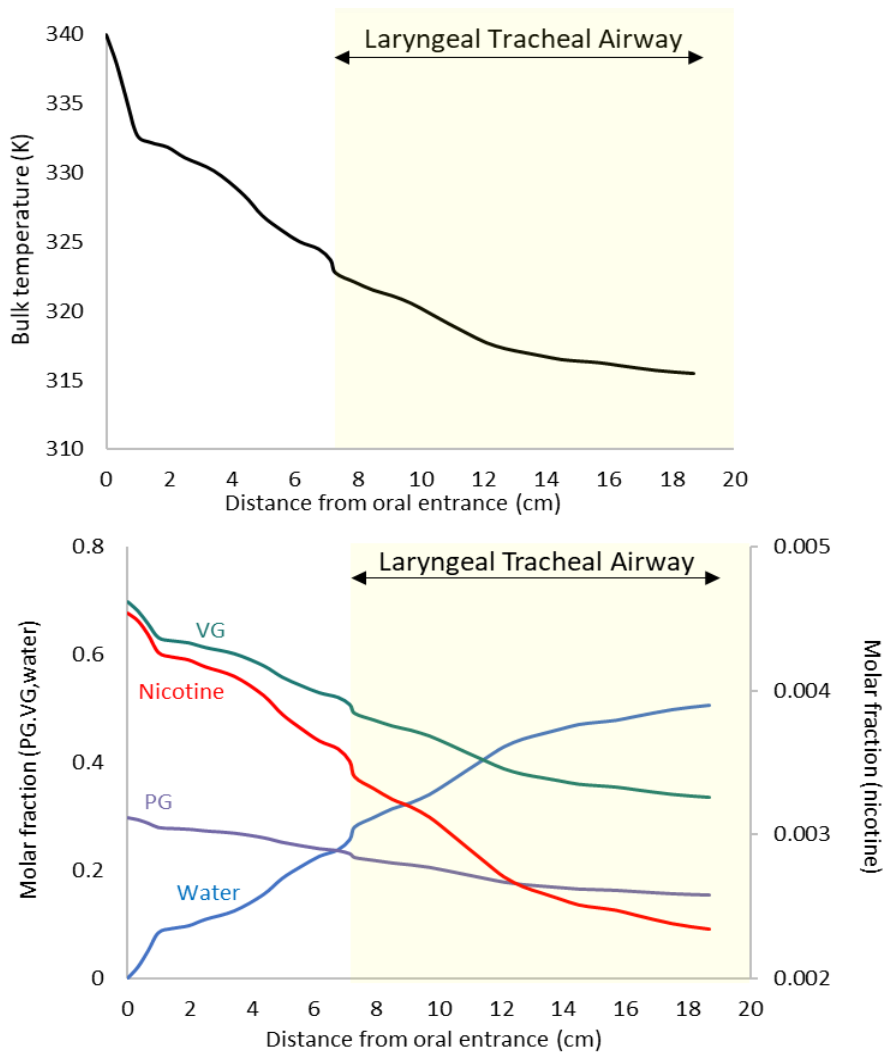


Figure 5: Aerosol temperature and particle phase molar fractions variation along the airway for condition A.

Throat nicotine vapor deposition increased with device power, nicotine concentration, freebase fraction and inhalation flow rate. An increase in nicotine concentration (i.e. molar fraction of nicotine in the particle phase) and freebase fraction leads to a higher nicotine vapor concentration entering the oral cavity as shown in equation (4). The higher molar fraction of nicotine also boosts the partial pressure of nicotine on the particle's surface, reducing the condensation potential of nicotine vapor from the aerosol. Further, the increase of throat nicotine vapor deposition with increasing flow rate results from higher values of the mass transfer coefficients in all airway sections.

At higher device powers, the temperature of the aerosol and the concentration of particles at the entrance of the oral cavity increase, leading to two outcomes. First, higher temperatures cause the vapor pressure of nicotine to rise, making more nicotine vapor available at the oral cavity entrance. Additionally, higher nicotine vapor pressures reduce the condensation of nicotine on the particles, as indicated by equations (3) and (4), allowing for higher nicotine vapor concentrations for absorption in the upper airway. Second, the rise in particle concentration decreases the dilution rate per particle as water and other aerosol components condense on the particle's surface.

The segmental nicotine vapor deposition rates per cm^2 of throat surface area for conditions A through E are illustrated in Figure 6. The first third of the laryngeal tracheal airway accounted for the highest nicotine deposition rates across the five simulated conditions and this can be attributed to higher nicotine vapor concentrations, nicotine molar fractions in the particle phase, and bulk temperatures as shown in figures 4 and 5.

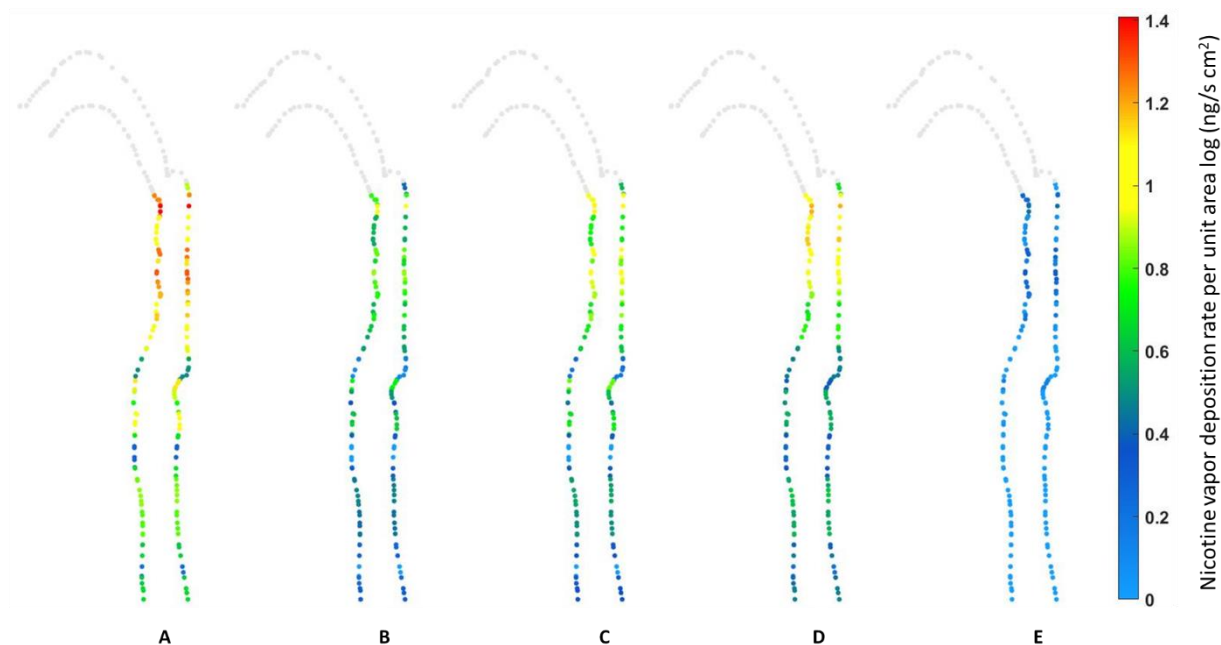


Figure 6: Predicted segmental nicotine vapor deposition rates per cm² of throat surface area at conditions shown in table 4.

1.3.2. Throat nicotine vapor deposition and throat hit

Figure 7 shows the reported subjective throat hit scores as a function of the model predicted nicotine vapor deposition per puff second. There was a significant positive correlation between reported subjective throat hit values and model predicted nicotine vapor deposition ($r=0.58$; $p<0.0001$) indicating that the developed model demonstrates the association of subjective throat hit with nicotine vapor deposition in the throat region. On the other hand there was no correlation between nicotine flux and subjective throat hit as illustrated in figure 8. Conditions with significantly higher nicotine flux using protonated nicotine exhibited significantly lower throat nicotine vapor rates compared to conditions where freebase nicotine was used showing that nicotine flux can be tuned independently from throat hit.

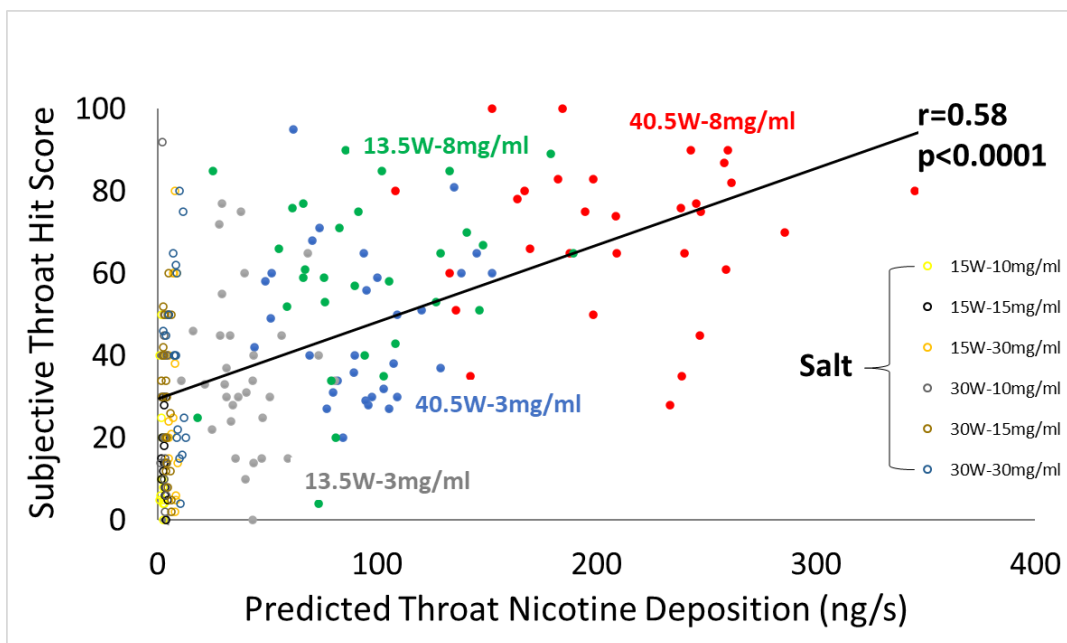


Figure 7: Subjective throat hit sensation vs model predicted throat hit flux for all conditions of studies of (S1) and (S2) – N=233

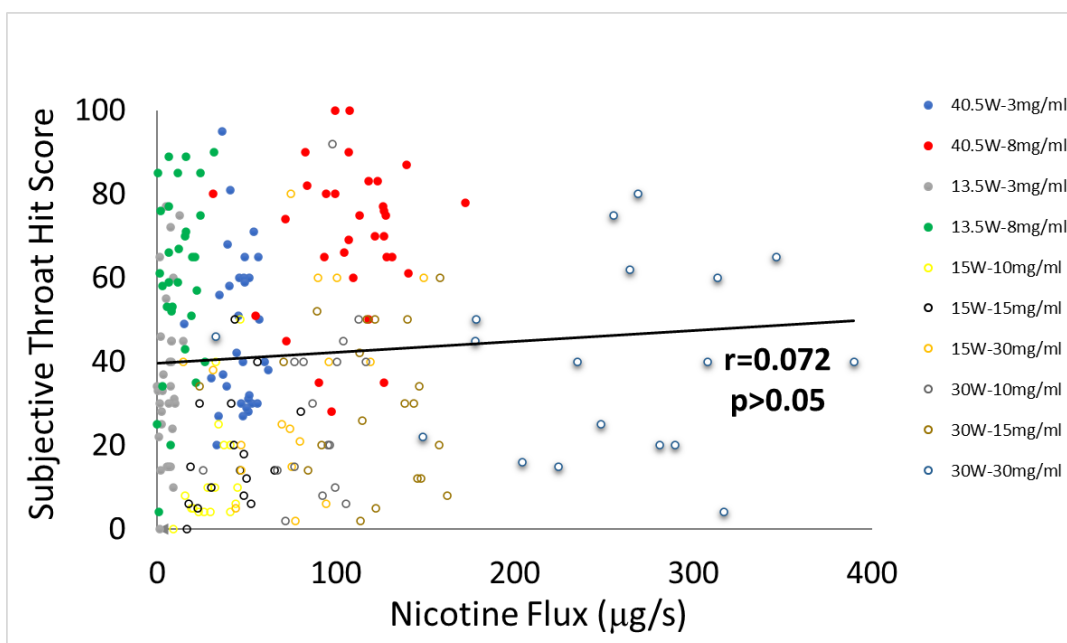


Figure 8: Subjective throat hit sensation vs model predicted nicotine flux for all conditions of studies of (S1) and (S2) – N=233

1.4. Conclusion

Throat hit resulting from the inhalation of ENDS aerosol can be reliably predicted using computer simulations and is the net outcome of the interplay of various

variables related to the device use conditions and user puff topography. Nicotine flux can be manipulated by ENDS manufacturers independently from throat hit allowing for products having high nicotine flux and relatively low throat hit readily available for people having low harshness tolerance like nicotine naïve youth. The developed model is a potential tool that can be used by regulators for convenient exploration of the interplay between ENDS properties and throat hit.

CHAPTER 2

DOES THE BUBBLER SCRUB KEY TOXICANTS FROM WATERPIPE TOBACCO SMOKE? MEASUREMENTS AND MODELING OF CO, NO, PAH, NICOTINE, AND PARTICULATE MATTER UPTAKE

2.1. Introduction

Waterpipe tobacco smoking (WTS) (aka narghile, hookah, shisha; see Figure 9) has been characterized as a global epidemic³⁶. Previous studies reported that a single waterpipe (WP) use session involves inhalation of large quantities of the same toxicants that are deemed responsible for dependence, cardiovascular disease, cancer, and pulmonary disease in cigarette smokers³⁷, and that regular WP users are prone to many acute and long term adverse health effects³⁸. Researchers attribute the appeal of this tobacco use method to the availability of a vast array of sweetened tobacco flavors³⁹, the social functions served by WP smoking particularly for youth⁴⁰, mega-marketing platforms such as the internet⁴¹, and a deficiency of WP-specific tobacco control measures⁴². Another reason given for its widespread popularity is the common perception that water bubbler filters the smoke from harmful constituents.^{43,44} To date, this perception has not been addressed head-on by a study quantifying the effect of the water bubbler on the major classes of toxicants found in WTS; such as study can support development of tobacco control messages directed to the public. In this study we compared nicotine, carbonyl compounds (CCs), polycyclic aromatic hydrocarbons (PAHs), NO, CO, and dry particulate matter (DPM) yields in WTS generated when the smoke traveled through the water bubbler and when it bypassed the bubbler. These

toxicants are among the major causative agents in cigarette smoking-related addiction, cancer, and cardiovascular and pulmonary diseases⁴⁵

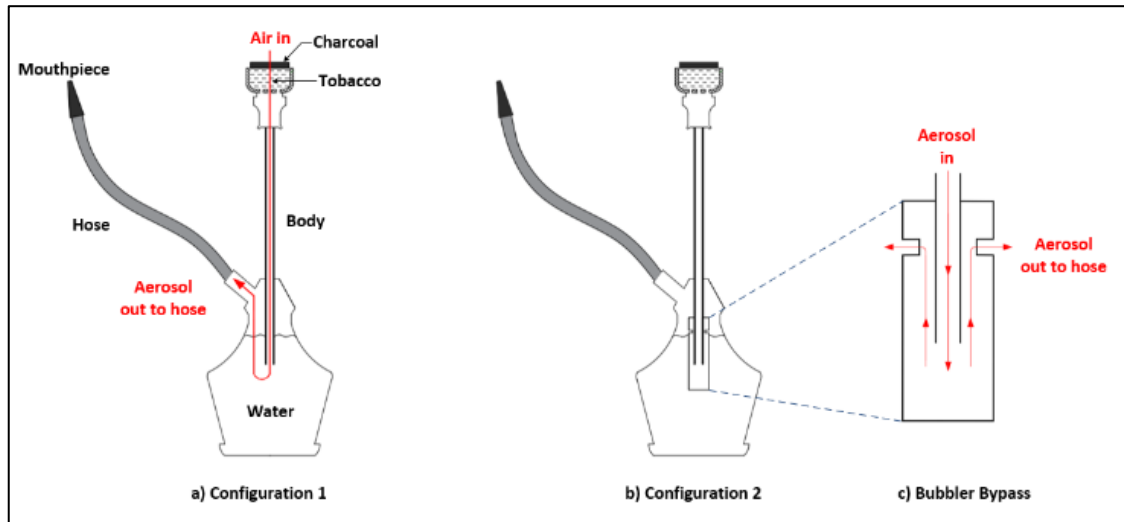


Figure 9: Schematic of a waterpipe a) unmodified, and b) configured such that the smoke bypasses the water bubbler.

2.2. Methods

2.2.1. Study design

We measured mouthpiece toxicant emissions for two different experimental conditions, each repeated 5 times in random order. In the first condition, a standard WP (Figure 9a) was used in which the smoke bubbled through the water. In the second condition (Figure 9b), a flow fitting was attached to the bubbler inlet, which allowed the smoke to bypass the water. The bypass fitting consisted of a cylindrical tube that was closed on one end; the other end contained four outlet ports that exhausted above the water line of the bubbler, allowing the smoke to travel directly to the hose without passing through the water (Figure 9c). This experimental approach allowed the dead volume in the waterpipe vase to remain constant across conditions.

2.2.2. Smoking machine protocol

We programmed a digitally controlled smoking machine⁴⁶ to generate smoke in accordance with the Beirut Method, which specifies 171 puffs of 2.6s duration, at a flow rate of 12.2 L/min, and with a 17 s interpuff interval⁴⁷. Further details about waterpipe preparation and charcoal application are provided in Shihadeh & Saleh (2005).⁴⁸ The waterpipe used in the study was manufactured by MYA (53 cm overall height, leather hose with infiltration rate of 1.8 liters per minute, when tested in accordance with Saleh & Shihadeh (2008)⁴⁹).

2.2.3. Sampling and analysis

We measured emissions included total particulate matter, DPM, nicotine, CO, NO, PAHs, and nine carbonyl compounds CCs. Particulate and gas-phase constituents exiting the waterpipe mouthpiece were measured directly online (nitric oxide) or trapped by a combination of particle filters, silica denuders, and grab sample bags and analyzed off-line, as described in Shihadeh et al. (2012)⁴⁸. Nicotine was quantified by GC-MS using standard procedures described in Siegmund et al. (1999)⁵⁰. PAHs were quantified using the methods described in Jawad et al.(2018).⁵¹ As described in Shihadeh et al. (2012)⁴⁸, CCs were trapped on DNPH-coated H10 cartridges for offline analysis using high-performance liquid chromatography–mass spectrometry (HPLC-MS), while NO and CO were measured using a rapid-response EcoChem CLD 70S chemiluminescence analyzer and electrochemical sensing, respectively. Karl-Fisher titration was used to determine particulate water content, as per Shihadeh and Saleh (2005)⁴⁶.

2.2.4. Statistical analysis

Outcome variables were summarized as mean (standard deviation). Independent student's t-test was used to indicate statistical significance between experimental conditions. $p < 0.05$ was taken as a significant difference.

2.2.5. Mathematical model description

The particle phase is assumed to consist of an ideal solution of glycerol, water, nicotine, and unresolved low volatility compounds initially in phase equilibrium with their surroundings. As the bubble is “released” into the column of water (modeled as a quiescent, infinite reservoir), diffusional mass transport driven by concentration gradients within the bubble is allowed to commence, as described by Fick's Law. At the bubble surface, a convection mass transfer formulation is employed. For water, the driving force for mass transfer is the high humidity (100%) of the gas layer immediately adjacent to the bubble surface relative to the vapor layer immediately adjacent to the aerosol particles, causing the aerosol particles to continually absorb water while they are trapped in the bubble. Conversely, the driving force for nicotine and glycerol transfer is the high concentration in the vapor layer adjacent to the aerosol particles, relative to that at the bubble surface. Thus, the water vapor and nicotine vapors diffuse in opposite directions, with the particles continually gaining water and losing nicotine and glycerol. At each time step, the composition of the vapors and particles are updated based on mass conservation and transport using a finite difference approximation of the transport equations. Mass transfer to/from the particle phase is modeled to account for non-continuum effects and unity mass accommodation is assumed. The numerical

simulation was validated against exact analytical solutions for the 1-D diffusion equation for a single component solution, as described by Friedlander (2000)⁵².

2.2.6. *Mathematical model governing equations*

When a waterpipe user draws a puff through the hose, the aerosol bubbles into the bowl. Inside every bubble, numerous physical phenomena occur as the bubble rises to the surface. First, gas molecules diffuse towards the surface of the bubble where they can be absorbed into the water, and subsequently mix with the water in the bowl, if a gradient in concentration exists between the bubble bulk and surface. The concentration gradient depends, among other things, on the gradient in pressure, temperature, and mole fraction of the individual species, i.e., molecules different than water may diffuse to the bubble surface which is assumed to be always fully saturated with water at ambient temperature. To estimate the temperature difference between the bubble bulk and surface, we used heat transfer modeling and found the aerosol temperature at the inlet pipe exit to be equal to 28.5°C. We then computed the mass transfer rate of gas molecules from the bulk to the bubble's surface using equation (12)²⁹:

$$\dot{m}_{v,i} = h_{m,i} A_s \Delta C_i \quad (12)$$

This transfer of molecules causes a perturbation in the initial gas equilibrium, which drives the molecules to evaporate or condense to restore equilibrium. The equilibrium profile of an aerosol undergoing phase change is given by equation (13):

$$\frac{dm_{p,i}}{dt} = 2\pi\Phi d_{p,i} D_{v,i} \frac{M_i}{R_u} \left(\frac{P_{vb,i}}{T_b} - \frac{K_R n_{f,i} P_{s,i}}{T_p} \right) \quad (13)$$

Where the Fuchs correction factor $\Phi = \frac{2\lambda + d_p}{d_p + 5.33 \left(\frac{\lambda^2}{d_p} \right) + 3.42\lambda}$ accounts for the non-

continuum effect of small particles approaching the mean free path λ of air molecules²⁸.

We estimated the aerosol distribution (N_{tot} , d_p) based on previous studies^{53,54}, and calculated $D_{v,i}$ using semi-empirical correlations²⁸.

To estimate the total number of timesteps needed for the simulation, we measured the time it takes for a bubble to rise to the surface of the water by filming the bubble ascent in slow-motion. We found the rise time of a bubble to be equal to 0.03s.

The modeled species are water, glycerin, nicotine, and benzo[a]pyrene. However, the model can be used to predict the behavior of any other toxicant of interest. Table 4 shows the model's initial input parameters.

| Parameter | Value |
|----------------------|--|
| x_{water} | 0.35 |
| $x_{glycerin}$ | 0.6449 |
| $x_{nicotine}$ | 0.005 |
| $x_{benzo[a]pyrene}$ | 0.0001 |
| d_p | 100 nm |
| d_B | 1 cm |
| N_0 | 3.5×10^6 particles/m ³ |

Table 4: The initial input parameters used in the model. x represents the initial mass fractions of the individual components. d_p and d_B are the particle and bubble diameters, respectively. N_0 is the initial number concentration of particles inside the bubble.

2.2.7. Numerical methods

We coded the model in the MATLAB computing environment using a forward Euler numerical scheme, with a time step of 0.3×10^{-5} s and assured time-step independence by running the model using a time step 0.3×10^{-6} s and obtaining similar results.

2.3. Results

There were no significant differences in total particulate matter (TPM), DPM, CO, NO, total PAHs, or tobacco consumed across the two conditions. However, bypassing the water bubbler resulted in significantly greater nicotine ($p < 0.01$) and CCs

($p < 0.0001$), but less water in the aerosol ($p < 0.01$). The results are detailed in Table 5 which also shows results from previous studies.

| Toxicant yield/session | Unmodified | Bubbler bypassed | Previous Studies |
|---|-------------------|-------------------------|---------------------------|
| Tobacco consumed, mg | 5284.7 (606.3) | 5449.3 (290.3) | 4700 (400) ⁴⁶ |
| Total particulate matter, mg | 1963.0 (177.4) | 1776.1 (134.1) | 1380 (260) ⁴⁶ |
| Dry particulate matter, mg | 1170 (80.6) | 1216.9 (113.9) | 909 (195) ⁵⁵ |
| Nicotine, mg | 4.2 (0.5) | 8.8 (2.5)* | 2.96 (-) ⁴⁶ |
| Carbon monoxide, mg | 213.4 (15.9) | 200.8 (26.6) | 197 (13.1) ⁵⁵ |
| Nitric oxide, μg | 655.6 (33.9) | 591.2 (71.1) | 280 (40) ⁵⁵ |
| Polyaromatic hydrocarbons, ng | | | |
| Naphthalene | 337.5 (77.5) | 286 (128.2) | 230 (64) ⁵⁵ |
| Acenaphthylene | 143.7 (31.8) | 97.5 (44.2) | 74 (13) ⁵⁵ |
| Acenaphthene | 49.7 (6.9) | 44.2 (21.2) | ND ⁵⁵ |
| Fluorene | 144.9 (30.4) | 91.2 (8.2)* | 437 (-) ⁵⁶ |
| Phenanthrene | 1046.5 (116) | 1107.6 (340.7) | 1185 (246) ⁵⁵ |
| Anthracene | 275.9 (55.9) | 243.5 (103.1) | 234 (44) ⁵⁵ |
| Fluoranthene | 749.3 (99.9) | 722.2 (268.3) | 639 (118) ⁵⁵ |
| Pyrene | 700.2 (82.9) | 659.7 (233.1) | 564 (103) ⁵⁵ |
| Benzo[a]anthracene | 69.9 (8.9) | 85.1 (35.9) | 130 (27) ⁵⁵ |
| Chrysene | 122.3 (19.1) | 126.6 (14.5) | 135 (24) ⁵⁵ |
| Benzo[b+k]fluoranthene | 83.2 (19.3) | 87.2 (32.2) | 72 (10) ⁵⁵ |
| Benzo[a]pyrene | 374.1 (75.3) | 431.8 (128.2) | 96 (21) ⁵⁵ |
| Benzo[g,h,i]perylene | 24.6 (3.9) | 34.3 (9.0) | 57 (10) ⁵⁵ |
| Dibenz[a,h]anthracene | 71.0 (9.6) | 59.6 (16.0) | 147 (-) ⁵⁶ |
| Indeno[1,2,3-cd]pyrene | 76.5 (11.5) | 56.4 (13.2)* | 69 (9) ⁵⁵ |
| Total PAHs | 4269.2 (551.5) | 4132.9 (1276.0) | - |
| Carbonyl compounds, μg | | | |
| Formaldehyde | 66.4 (34.4) | 103.4 (24.6) | 36.0 (6.25) ⁵⁵ |
| Acetaldehyde | 633.4 (116.0) | 1387.3 (136.8)* | 492 (88) ⁵⁵ |
| Acetone | 219.6 (54.4) | 648.5 (64.2)* | 118 (-) ⁴⁸ |
| Acrolein | ND | 11.5 (12.6) | ND ⁵⁵ |
| Propionaldehyde | 104.7 (17.5) | 200.6 (39.5)* | 92.9 (16.7) ⁵⁵ |
| Crotonaldehyde | 10.8 (0.05) | 25.7 (8.8)* | 73.7 (10.8) ⁵⁴ |
| Methacrolein | 13.3 (4.4) | 34.3 (5.0)* | 19.9 (2.63) ⁵⁵ |
| Butyraldehyde | 84.8 (7.8) | 109.6 (8.1)* | 68.8 (16.9) ⁵⁴ |
| Valeraldehyde | 64.8 (9.8) | 69.4 (28.9) | 4.3 (7.4) ⁵⁴ |
| Total CCs | 1197.9 (179.0) | 2590.2 (293.0)* | - |

Table 5: Toxicant yields [mean (standard deviation)] for N=5 repeated sessions for each condition. * indicates statistically significant difference relative to baseline condition. ND indicates below instrument detection limits.

2.4. Discussion

In this study, we investigated the effect of the water bubbler on WP smoke toxicant content, and by doing so, addressed directly a widely-held perception among users that the bubbler effectively filters the smoke. We also developed a mathematical model representing the mass transfer from a multicomponent internally mixed aerosol to help interpret the measurements. We found that the water bubbler had no measurable effect on DPM, CO, NO, and PAH, major probable causative agents in cardiovascular disease, chronic obstructive pulmonary disease (COPD), and lung and larynx cancer in cigarette smokers⁵⁷. On the other hand, the water bubbler was found to reduce smoke nicotine and total CCs content each by approximately 50%. Nicotine is the major causative agent in addiction, and – along with CO, NO, DPM, and PAH – CCs are implicated in COPD. While total CCs were reduced by 50% by the bubbler, valeraldehyde, did not display any significant variation between the two conditions. This can be attributed to the low solubility of valeraldehyde in water⁵⁸. The observed differences across conditions in nicotine and CCs but not CO, DPM, or other particle phase components may seem contradictory. However, the observations are consistent with a picture in which species that are both volatile and water soluble (e.g. nicotine, CCs) are absorbed to some extent into the water, while species that are either non-volatile (e.g. BaP) or volatile but negligibly soluble (e.g. CO) are not absorbed or deposited into the water bubbler. We observed this behavior in computer simulations of a multicomponent aerosol trapped in a bubble rising through a 3 cm column of water. Figure 10 shows a computer simulation of the evolving composition of a hypothetical aerosol system composed of glycerin, nicotine, water, and benzo(a)pyrene as it rises through the water. Glycerin and benzo(a)pyrene, both of which are of low volatility,

remain constant, while, on the other hand, the relatively high volatility and water-soluble nicotine is transferred out of the aerosol. Interestingly, also corroborating the experimental observations summarized in Table 5, the simulations predict water transfer into the aerosol as the particles scavenge water vapor from their surroundings. Thus, the observed differential effects of the water bubbler on water, nicotine and CCs smoke content on the one hand, versus DPM, CO, NO, PAH, on the other, are well-described by theory. All in all, the experimental findings were consistent with a picture of mass transfer that is driven by gas-phase diffusion processes, and minimal particle deposition. Unfortunately for waterpipe smokers, this means that the bubbler has little filtering effect except for species that are volatile and water soluble. Also, although bubbling resulted in a 50% reduction in nicotine and CCs, levels of these toxicants reaching the user remain high.

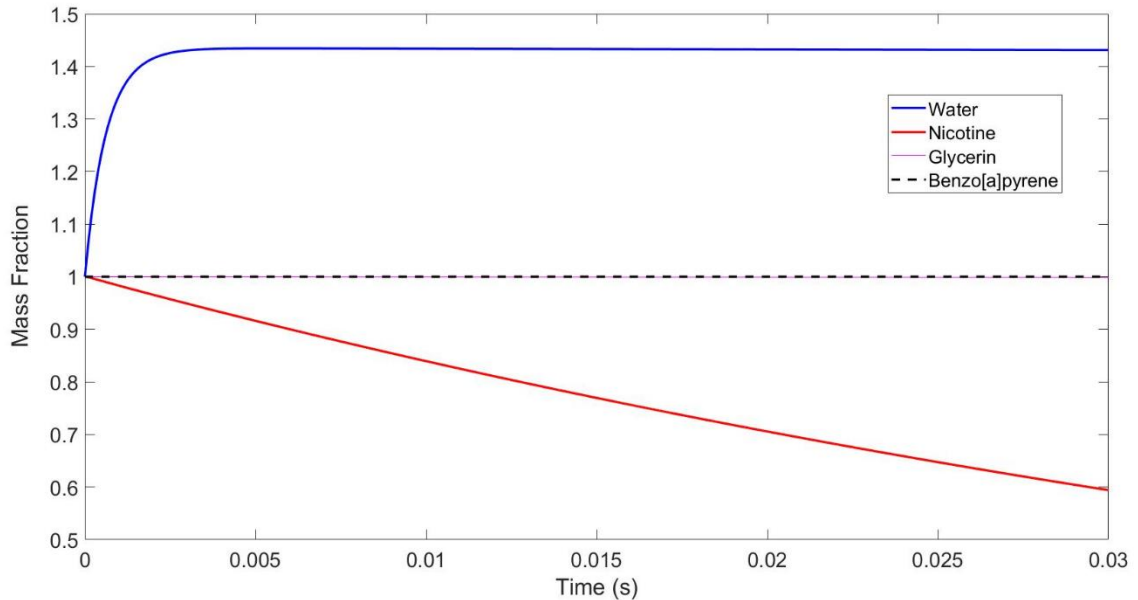


Figure 10: Simulation results showing evolution of component mass relative to initial mass for a hypothetical aerosol consisting of water, glycerin, nicotine, and benzo(a)pyrene trapped in a 1 cm bubble rising through a 3 cm column of water at 25 °C. Initial aerosol conditions: 3.5×10^6 particles/m³, particle diameter: 100 nm.

2.5. Conclusion

In conclusion, the widespread perception that water bubbling filters WP smoke is misleading. We found that the WP bubbler does not significantly reduce PAH, CO, NO, or DPM – major classes of toxicants that are implicated in cardiovascular disease, COPD, and lung and larynx cancer in cigarette smokers. While the bubbler does reduce nicotine and CCs by approximately 50%, yields of these toxicants are still high, in some cases much higher than yields from a single cigarette.

CHAPTER 3

COMPARISON OF CO, PAH, NICOTINE, AND ALDEHYDE EMISSIONS IN WATERPIPE TOBACCO SMOKE GENERATED USING ELECTRICAL AND CHARCOAL HEATING METHODS

3.1. Introduction

Waterpipe tobacco smoking (aka “shisha,” “hooka”, “argileh”) has become a global phenomenon⁵⁹. Its popularity is reflected in the volume of online searches of waterpipe products especially in the United States where a relative increase of more than 60% was observed between 2004 and 2013⁴¹. Youth appear to be particularly prolific consumers of waterpipes. For example, in Canada the peak age group prevalence ranges between 18 and 24⁶⁰. Importantly, a large population of waterpipe smokers perceive it as less harmful than cigarettes^{61,62}. This perception of lower harm is not supported by the available evidence; waterpipe tobacco smoke contains high concentrations of the toxicants in cigarette smoke and that are associated with various diseases including cancer^{55,63-68}. Several of these toxicants, measured using analytical lab studies, have also been found in the urine, breath and blood of waterpipe smokers^{68,69}.

Waterpipe tobacco smoking involves the use of burning charcoal as the heat source. It is placed on top of a tobacco preparation known as ma’ssel, an Arabic word for honey⁷⁰. Ma’ssel is a mixture of tobacco, glycerin, water, and flavorants⁷⁰. It began to be widely marketed in the 1990s⁷¹ and is highly popular among users today. Some users smoke an un-flavored tobacco commonly known as jurak, or ajami, which is prepared by partially

soaking the tobacco in water. In this use configuration, charcoal is placed directly on the tobacco without any foil separation⁷².

By weight, typically more charcoal is consumed during a smoking session than is tobacco⁷³. It has been shown previously that charcoal accounts for approximately 90% of the CO and carcinogenic PAHs emissions in WTS⁶³ and that levels of plasma nicotine, CO boost, heart rate and exhaled benzene were significantly lower when waterpipes were smoked in a clinical laboratory using an electric heater in place of the charcoal⁷⁴. In recent years, electrical heating elements (EHEs) have become commercially available, allowing users to smoke without charcoal. EHEs commonly allow the user to select from a range of electrical power inputs. Package labeling and online vendors advertise them as “toxicant free” and “carbon monoxide free”. Online customer reviews indicate that while some customers are pleased with these products, others complain that not enough smoke is generated, or that the tobacco is overheated⁷⁵. Some online reviews indicate the perception that using EHEs results in a lower smoke toxicity compared to conventional charcoal heating⁷⁶.

In theory, if EHEs are found to reduce exposure to harmful constituents in first or second-hand waterpipe tobacco smoke, regulations could be devised which prohibit the use of charcoal when waterpipes are served (e.g. in waterpipe cafés) and which monitor statements of harm used to advertise and promote tobacco heating sources. In this study, we investigated the thermal performance of three commercially available EHEs and compared emissions of several major toxicants in WTS generated using EHEs to those generated using charcoal. We note that EHEs are not the same as so called “e-hookah”, which, like an electronic cigarette, employs an electrical heater to heat and vaporize a flavored, nicotine-containing liquid.

3.2. Methods

3.2.1. Experimental procedures

This study was conducted in two phases. First, since the EHEs are powered by a variable power supply, the optimal operating power of each EHE needed to be determined. Second, WTS was generated using charcoal and each of the EHEs operating at its optimal power. Each condition was repeated in triplicate, and the WTS for each repeat was separately sampled and analyzed for TPM, PAHs, CCs, nicotine and CO.

3.2.2. EHE devices

The electric heating elements used are shown in Table 6. EHE-1 is made of ceramic and is placed directly over a traditional waterpipe head in place of charcoal. EHE-2 is a ceramic head with a built-in electrical heater. Once powered, the entire head heats the tobacco from the bottom up, in contrast to charcoal which heats the tobacco from the top-down. EHE-3 is made of metal and is set up similarly to a traditional waterpipe. The electric heating element is in a hinged cap that is placed on top of the head, directly above the tobacco.

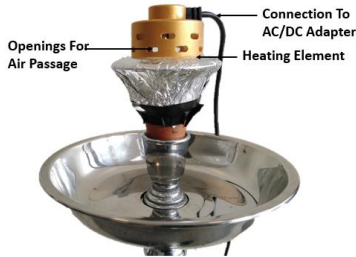

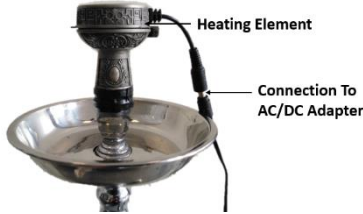
| Electric Heating Element | Tag | Manufacturer | Material | Resistance (Ω) | Power Range (W) |
|--|-------|-----------------------------|----------|-------------------------|-----------------|
|  | EHE-1 | “Ren Headstream” (China) | Ceramic | 3 | 49.5-79.6 |
|  | EHE-2 | “Ren Headstream” (China) | Ceramic | 2.95 | 72.4-117.1 |
|  | EHE-3 | “Hady” (China) | Metal | 2.5 | 37.7-74.4 |

Table 6: Schematic representation of the EHEs used in this study, in addition to their material properties and operation range.

3.2.3. Optimal power determination

Each of the EHEs allows the user to select from a range of electrical power output. For an apples-apples comparison, it was necessary to determine the “optimal” power at which each EHE would most closely mimic the performance of the charcoal. The selected performance metrics were the mass of tobacco consumed during a smoking session, and the TPM emitted per unit tobacco consumed (or the “yield ratio”). The first metric indicates the total thermal energy delivered to the tobacco, while the second metric is a measure of the relative importance of thermal conduction heating versus convective heat transfer by heated air. The former mode of heat transfer

emphasizes vaporization of the tobacco preparation through the top of the waterpipe head and into the environment between puffs, while the latter mode emphasizes vaporization during puffing. Vaporization during puffing results in a greater proportion of the vaporized components being carried into the puff bolus that reaches the mouthpiece. For example, a heating device that continuously heats the tobacco may result in a similar tobacco consumed outcome as charcoal, while producing very little aerosol at the mouthpiece. A more detailed description of heat transfer phenomena in the waterpipe head can be found in Monzer et al.⁶³.

For each EHE, ten equally spaced power settings were investigated, spanning the minimum to the maximum power for each device, and the tobacco burned and TPM emitted were measured. For each EHE, the power setting resulting in the yield ratio closest to that of the charcoal condition was defined as the optimum.

3.2.4. Machine smoking and toxicant sampling protocol

The waterpipe was smoked using a digitally controlled automatic smoking machine operating under the reduced Beirut smoking protocol: 105 puffs, 530 ml puff volume, 17 s interpuff interval, and 2.6 s puff duration^{46,47}. For each smoking session (charcoal or EHE), the bowl was filled with 850 ml of water and an infiltration test was performed on the leather hose to insure that the air infiltration was within the accepted tolerance of 1.5 to 1.7 L/min at a mouthpiece flowrate of 12.2 L/min; see Saleh and Shihadeh⁴⁹ for details. Then, 10 g of flavored tobacco (Two Apples, Nakhle brand) were placed in the head and covered by aluminum foil perforated according to a predefined 18-hole pattern⁷³. The head was then weighed and placed on the waterpipe body; electrical insulation tape was used to seal all joints in the waterpipe to avoid

uncontrolled air leakage. For the charcoal condition, one 33 mm diameter quick lighting charcoal briquette (Three Kings Charcoal Co., Holland) was used in each session. The charcoal was lit and held in metal tongs for one minute prior to placing it on the waterpipe head. For smoking sessions using electrical heating, the adjustable power supply was set to the optimal voltage for each EHE.

During each puff, the smoke exiting the mouthpiece was divided into two parallel flow streams, each passing through a 47mm glass fiber filter (Gelman type A/E) where the particle phase of the smoke was trapped. Filters were replaced periodically during the smoking session in order to avoid overload⁴⁶. The filters were weighed before and after sampling for TPM quantification and were stored in airtight containers in the dark at 3°C until extraction for nicotine and PAH analyses. Sixteen PAH compounds (Naphthalene, Acenaphthylene, Acenaphthene, Fluorene, Phenanthrene, Pyrene, benzo[a]anthracene, Chrysene, Benzo[k]fluoranthene, Benzo[b]fluoranthene, Benzo[a]pyrene, Benzo[g,h,i]perylene, Dibenz[a,h]anthracene, and Indeno[1,2,3-cd]pyrene) were quantified using the method described by Jawad et al.⁵¹ with an instrumental LOD (limit of detection) ranging from 1.35 to 1.5 ng and a LOQ (limit of quantification) ranging from 6 to 7.5 ng depending on the specific PAH. Nicotine concentration was determined by GC–MS following standard procedures presented in Talih et al.⁷⁷

Downstream of the particulate filters, a portion of the flow was diverted through a DNPH-coated silica cartridge to sample and derivatize CC species for offline analysis⁷⁸, and into an inert sampling bag for offline CO quantification by electrochemical sensor (Bacharach Monoxor III).

CC emissions in the gas phase of the smoke were trapped on DNPH-coated H30 cartridges (Lp-DNPH, Supelco). After collection, these cartridges were eluted with 10 ml of ethanol/acetonitrile (90/10 ratio)⁷⁹ and delivered into amber vials. All samples were analyzed by high-performance liquid chromatography-mass spectrometry (HPLC-MS; LC/MSD Trap XCT, Agilent Technologies, Santa Clara, CA, USA) equipped with a photodiode array detector at $\lambda=360$ nm, and at a flowrate of 1 ml/min. The analytes were detected based on their retention times compared to calibration standards. Gradient elution on a reverse phase C-18 column (25 cm, 4.6 mm, 5 μ m) was performed. The solvents used were (A) water/ACN/ THF (6:3:1 v/v/v), (B) water/ACN (2:3 v/v), and (C) ACN. The elution profile varied linearly in time from pure A at t=0 min to 25:75 A:B at t=20 min and finally to pure C at t=35 min. The instrumental LOD ranged from 0.001 to 0.006 μ g, and the LOQ ranged from 0.005 to 0.019 μ g depending on the specific CC⁸⁰.

3.2.5. Statistical analysis

Outcome variables including thermal performance parameters and toxicants were summarized as mean (standard deviation). Dependent (outcome) variables were compared based on heating source using one-way analysis of variance including post-hoc pairwise comparisons (Bonferroni). $p < 0.05$ was used to indicate statistical significance. SPSS version 24.0 (IBM, Armonk, NY) was used to perform the statistical analyses.

3.3. Results

The thermal performance, CO, nicotine PAHs, and CC yields of the three EHEs and charcoal are summarized in Table 7. The optimal power for the EHE's was found to range between 50 and 80 W. Yield ratio for EHE-2 and EHE-3 were not significantly different from charcoal when operated at powers of 77.3 and 50.2 W, respectively. On the other hand, at all powers tested, EHE-1 was incapable of reaching the yield ratio of charcoal. For EHE-1, the minimum difference with respect to charcoal was at the maximum power setting.

EHEs resulted in approximately a 90% reduction in CO and an 80% reduction in total PAH emissions relative to the charcoal condition. Nicotine yields were approximately 20% lower for EHE-1 and EHE-3, while EHE-2 was not significantly different than the charcoal condition.

Benzo[a]pyrene and total PAHs yields were significantly lower for all three EHEs compared to charcoal. Benzo[a]pyrene is listed as a Class 1 carcinogen by the International Agency for Research on Cancer (IARC 2018).

Acrolein, a highly reactive irritant thought to be responsible for nearly all the non-cancer respiratory disease risk associated with cigarette smoking⁸¹ was orders of magnitude greater for all EHEs relative to charcoal. Furthermore, none of the twelve quantified CC species was significantly greater for charcoal than for any of the EHEs; whenever a significant difference occurred, EHE emissions of CCs were always greater. Total CCs were not significantly different for EHE-1 and EHE-2 relative to charcoal, while a significant increase of 57% in total CC yield was observed for EHE-3. While total CCs for EHE-1 and -2 were not significantly different than charcoal, it is possible that a greater number of samples would have resulted in significant differences. Indeed,

an independent 2-factor analysis comparing EHEs to charcoal showed that total CCs were significantly higher ($p < 0.05$).

Results from the post-hoc analysis showed no significant difference between PAHs and nicotine yields amongst three EHEs, while CCs and CO yields were significantly different between EHE-2 and EHE-3.

| | Charcoal | EHE-1 | EHE-2 | EHE-3 |
|--|-----------------|----------------|----------------|----------------|
| Optimal power, W | - | 79.6 | 77.3 | 50.2 |
| Thermal performance | | | | |
| Tobacco consumed, mg | 4034.8 (260.9) | 4149.3 (48.0) | 4911.5 (473.5) | 3848.6 (46.7) |
| TPM, mg | 969.8 (169.2) | 655.8 (83.2) | 1080.6 (154.1) | 850.1 (49.4) |
| Yield ratio | 0.24 (0.031) | 0.16 (0.018)* | 0.22(0.013) | 0.22 (0.015) |
| Toxicant yields per session | | | | |
| Nicotine, mg | 5.4 (0.32) | 4.43 (0.34)* | 5.02 (0.64) | 4.18 (0.26)* |
| Carbon Monoxide, mg | 86.2 (4.6) | 6.2 (0.7)* | 4.7 (0.6)* | 6.3 (0.4)* |
| PAHs, ng | | | | |
| Naphthalene ^c | 98.5 (100.7) | 14.2 (3.9) | 18.8 (24.5) | 46.7 (72.4) |
| Acenaphthylene | ND | 14.9 (12.9) | ND | 13.3 (11.6) |
| Acenaphthene | 40.6 (30.5) | 27.4 (9.2) | 25.7 (8.1) | 59.8 (7.0) |
| Fluorene | 79.3 (71.5) | 10.5 (9.1) | NQ | 6.0 (10.4) |
| Phenanthrene | 876.5 (328.5) | 169.7 (30.0) | 113.2 (34.7) | 149.1 (28.3) |
| Anthracene | 148.6 (43.1) | 24.0 (6.9)* | 7.7 (8.2)* | 48.7 (40.8)* |
| Fluoranthene | 707.5 (101.6) | 140.4 (33.7)* | 92.4 (24.5)* | 94.7 (3.8)* |
| Pyrene | 611.2 (82.8) | 93.4 (18.3)* | 71.7 (26.5)* | 73.10 (6.8)* |
| Benzo[a]anthracene ^c | 88.7 (25.3) | ND* | ND* | ND* |
| Chrysene ^c | 157.6 (26.3) | 16.7 (2.1) * | 49.7 (30.1)* | 9.9 (8.6)* |
| Benzo[k]Fluoranthene ^c | 47.3 (10.9) | ND* | ND* | ND* |
| Benzo[b]Fluoranthene ^c | ND | ND | ND | ND |
| Benzo[a]pyrene ^a | 98.8 (14.7) | 18.9 (32.7) * | 46.2 (17.2)* | 37.8 (16.6)* |
| Benzo[g,h,i]perylene | ND | ND | ND | ND |
| Dibenz[a,h]anthracene ^b | ND | ND | ND | ND |
| Indeno[1,2,3-cd]pyrene ^c | ND | ND | ND | ND |
| Total PAHs | 2954.5 (565.0) | 530.1 (67.6)* | 425.4 (108.5)* | 539.0 (28.8)* |
| Carbonyl Compounds, µg | | | | |
| Formaldehyde ^a | 12.2 (3.0) | 20.0 (1.5)* | 18.7 (4.3) | 25.0 (7.1) |
| Acetaldehyde ^c | 579.8 (114.6) | 1015.0 (71.5)* | 761.6 (26.9) | 1101.0 (79)* |
| Acetone | 429.3 (42.4) | 385.0 (7.6) | 376.8 (9.2) | 494.0 (33.4) |
| Acrolein | ND | 14.1 (1.2)* | 16.6 (1.3)* | 14.4 (0.8)* |
| Propionaldehyde | 66.5 (17.6) | 67.9 (3.7) | 41.1 (3.1) | 86.1 (17.9) |
| Crotonaldehyde | 73.7 (10.8) | ND* | ND* | ND* |
| Methacrolein | 89.8 (5.3) | 88.6 (1.1) | 92.3 (0.9) | 98.6 (2.1) |
| Butyraldehyde | 68.8 (16.9) | 67.5 (4.3) | 63.7 (1.4) | 94.1 (7.5) |
| Benzaldehyde | ND | ND | ND | ND |
| Valeraldehyde | 4.3 (7.4) | ND | 19.7 (4.8) * | 76.8 (72.5) |
| Glyoxal | 8.7 (0.4) | 10.2 (3.1) | 8.7 (1.0) | 11.0 (1.9) |
| Methylglyoxal | 157.1 (45.3) | 187.4 (111.7) | 277.1 (98.7) | 336.1 (94.9) |
| Total CCs | 1490.3 (177.8) | 1855.7 (177.9) | 1676.3 (113.7) | 2337 (183.4) * |

* Significant statistical difference compared to charcoal ($p < 0.05$)

^a Carcinogenic to humans according to IARC list of classifications, volumes 1-121 (2018)

^b Probably carcinogenic to humans according to IARC list of classifications, volumes 1-121 (2018)

^c Possibly carcinogenic to humans according to IARC list of classifications, volumes 1-121 (2018)

ND: Below detection limits

NQ: Below quantifiable limits

Table 7: Thermal performance, CO, Nicotine, PAHs and CCs yields [mean (standard deviation)] for N=3 smoking sessions according to the reduced Beirut smoking protocol.

3.4. Discussion

This study aimed at assessing the thermal performance of three commercially available waterpipe electric heating elements and quantifying their toxicants emissions relative to conventional charcoal. Limitations of this study include the use of a single flavor and brand of tobacco (i.e. there was no variation in the concentration of components present in the tobacco), and a single type of charcoal. Another limitation is that EHE performance was evaluated strictly by analytical laboratory criteria rather than user experience.

Two of the three tested electric heating elements (EHE-2 & EHE-3) were capable of attaining thermal performance characteristics similar to charcoal. Their yield ratios of 0.22 were the same as reported by Monzer et al. (2008) for an experimental heating element that was carefully designed to mimic spatial and temporal heating characteristics of charcoal. For all EHE's the average nicotine yield was similar to that of charcoal. Thus, in terms of amount of tobacco burned, the density of the generated aerosol, and the nicotine yield, commercially available EHE's appear capable of providing charcoal-like performance. Also consistent with Monzer et al.⁶³ and Brinkman et al.⁷⁴ replacing charcoal by an EHE greatly reduced CO and PAH emissions in the mainstream aerosol. On the other hand, EHEs resulted in an increase in CC emissions, including acrolein, the primary causative agent in non-cancer respiratory disease in cigarette smokers. The elevated CC emissions from EHEs may be intrinsic to the constant power output of these devices. That is, during and between puffs, the

electric power is constantly on. As a result, conduction heat transfer between the EHE and the tobacco may result in greater heating between puffs, and higher tobacco temperatures in the direct vicinity of the heating surface, where charring occurs⁶³. These higher temperatures would, in turn, result in greater thermal degradation of the tobacco and vegetable glycerin (VG) making up the *ma'ssel*, and greater production of CC species. Thermal degradation of propylene glycol and VG by electrical heating has been widely reported in studies of electronic cigarettes⁸²⁻⁸⁴. In contrast, charcoal combustion is a function of ventilation rate; whenever a puff is executed, the charcoal visibly glows red, and a bolus of hot air and combustion products is drawn through the tobacco to generate the aerosol. Heating between puffs is relatively modulated by the slower combustion rate. Another hypothesis for the lower CC yields when waterpipes were smoked using charcoal is that constituents (e.g. free radicals) produced by the burning charcoal may have reacted with the CCs and resulted in their destruction.

3.5. Conclusion

In conclusion, EHEs can result in similar quantities of aerosolized particulate matter and nicotine as charcoal. The combustion-related toxicants CO and PAH are greatly reduced when EHEs substitute charcoal. On the other hand, this electrical heating modality can greatly increase emissions of acrolein, a major causative agent in non-cancer respiratory disease. These mixed findings underscore the complexity of toxicant reduction by tobacco product design manipulation and suggest that marketing EHEs as reduced harm products may be misleading.

CHAPTER 4

COMPARISON OF NICOTINE EMISSIONS RATE, “NICOTINE FLUX”, FROM HEATED, ELECTRONIC, AND COMBUSTIBLE TOBACCO PRODUCTS: DATA, TRENDS, AND RECOMMENDATIONS FOR REGULATION

4.1. Introduction

Despite decades of tobacco control efforts, tobacco smoking remains one of the leading causes of premature death globally, estimated at 8 million deaths per year, and a major threat to public health⁸⁵. The psychomotor stimulant nicotine is the main addictive agent in tobacco smoke and, without it, tobacco consumption would not be sustained^{14,15}. As with other abused drugs, the dose and the speed at which nicotine reaches brain are critical to producing the addictive character of tobacco smoking⁸⁶. In principle, more rapid delivery and greater dose result in greater reinforcement and greater abuse liability⁸⁷. One reason combustible cigarettes are addictive is that inhaled tobacco smoke delivers nicotine to the brain in seconds, more rapidly even than intravenous nicotine delivery¹⁶. Historically, nicotine yield has served as the metric for characterizing the amount of nicotine emitted by different combustible cigarette products⁸⁸. Yield is defined as the mass of nicotine emitted through the mouth end of a tobacco product per unit of consumption (e.g., milligrams of nicotine per cigarette; mg/cig). The rate at which nicotine is delivered, the yield per unit time, is referred to as the “nicotine flux” (mg/s or $\mu\text{g/s}$)⁸⁹. Because combustible cigarettes are made in a standard size, and are consumed in roughly five minutes, nicotine yield and nicotine

flux are closely coupled with combustible cigarettes – a cigarette with a high yield will also have a high flux.

On the other hand, with electronic nicotine delivery systems (ENDS) and other products whose use patterns vary widely, the yield and the flux are not coupled closely. A product may have low yield and high flux (e.g., the one-puff “dokha”⁹⁰) or vice-versa (e.g., nicotine patch). Typically, an ENDS product is consumed during multiple use sessions spanning a period of one to several days, depending on such factors as the size of the reservoir containing the nicotine solution and the electrical power of the device. Therefore, the nicotine yield of the product per unit sold may not be relevant to the yield obtained during a single use session. For example, a single JUUL pod emits roughly the same amount of nicotine as an entire pack of cigarettes but is unlikely to be consumed entirely in a single-use session⁹¹. Even the notion of a use session for an ENDS product may be difficult to define. Does taking a single puff just before entering an office building constitute a “session”? Nicotine patches, too, can deliver a dose of nicotine over a day that is comparable to a pack of cigarettes. Clearly, a comparison of the yield of a JUUL pod, a nicotine patch, and a cigarette stick has little value because the consumption patterns differ greatly; as a regulatory target, yield is not a useful construct. Nicotine flux, on the other hand, allows comparisons across products and product classes because it normalizes nicotine emission by time. In doing so, flux also highlights the key factor of speed of delivery: nicotine flux is the theoretical upper limit of the rate at which nicotine can reach the brain. As we have discussed elsewhere⁹², to be enforceable a flux standard implies that only closed systems will be allowed on the market.

Figure 11 illustrates by analogy the relationship between nicotine flux, liquid nicotine concentration, device power, time, and nicotine yield for ENDS products. The large tank can be thought of as the liquid reservoir of an ENDS product, while the small container can be considered the mouth of the user. The nicotine concentration of the liquid in the tank was prepared by dissolving a given mass, m , of nicotine (mg) in a given volume, V , of liquid (mL), resulting in a liquid nicotine concentration $C = m/V$ (mg/mL). When a puff is executed, the rate at which liquid is aerosolized by the ENDS device (i.e., in the form of an inhalable aerosol) and delivered to the mouth of the user is represented by opening the tap, allowing the flow to commence at some rate Q (mL/s). The nicotine flux is the product of the nicotine concentration C and the volume flow rate Q . To a close first approximation, Q is directly proportional to the power (P , Watts); greater power translates to a more open tap in Fig 11. As a result, nicotine flux is directly proportional to the product of C and P . Finally, the amount of nicotine collected from the tap while the valve was open is the yield, which is simply the product of the flux and time.

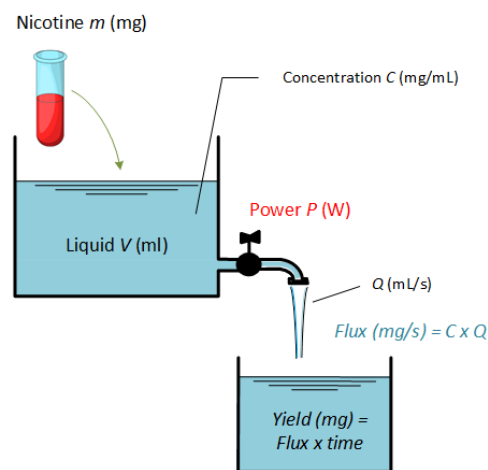


Figure 11: Relationship between liquid nicotine concentration, device power, flux (nicotine emission rate), and yield for an ENDS device by analogy to a reservoir emptying into a container through a valve and tap assembly. In this analogy, the electrical power of the ENDS device determines the degree to which the tap is open during a puff; greater power means a more open valve.

In this study, we sought to estimate nicotine flux for a wide range of tobacco products to provide a base against which a potential ENDS product regulation could be considered. To date, extant EU and proposed US regulations have focused exclusively on limiting liquid nicotine concentration, an approach which, counter to the stated aims of those regulations, constrains neither yield nor flux, and therefore does not constrain exposure (i.e., nicotine dose inhaled by the user).

4.2. Methods

Nicotine flux can be computed from published reports on tobacco product yields as the ratio of the yield to the cumulative puffing time of an inhaled tobacco product (e.g., a cigarette or pipe) or as the ratio of the yield to the cumulative time of use of a product that emits nicotine continuously (e.g., a nicotine patch).

For inhaled products, we searched the Scopus database using the following Boolean expression: ("nicotine" OR "nicotine yield") AND ("flow rate" OR "puff duration" OR "interpuff interval" OR "puff volume" OR "topography"). The search resulted in 651 documents, of which 39 reported values of nicotine yield, puff duration, and number of puffs; these 39 documents were retained for analysis.

The nicotine flux was computed as:

$$\text{Nicotine flux } \left(\frac{\mu\text{g}}{\text{s}} \right) = 1000 * \frac{\text{Nicotine yield } \left(\frac{\text{mg}}{\text{unit}} \right)}{\text{Total puff number } \left(\frac{\text{puffs}}{\text{unit}} \right) * \text{puff duration } \left(\frac{\text{s}}{\text{puff}} \right)} \quad (14)$$

For patch and gum products, we computed the flux as:

$$\text{Nicotine flux } \left(\frac{\mu\text{g}}{\text{s}} \right) = 1000 * \frac{\text{Nicotine dose } \left(\frac{\text{mg}}{\text{unit}} \right)}{\text{Total time of consumption } \left(\frac{\text{s}}{\text{unit}} \right)} \quad (15)$$

where the time of consumption was taken as 24 h for patches and 30 min for gum. The dose was taken as that provided by the manufacturer assuming complete release of nicotine during the time of product consumption.

Average (standard deviations) of nicotine fluxes for each tobacco product were determined to compare different products. A simple linear regression was used to test the correlation between year of publication vs. nicotine flux. Statistical significance was taken as $p < 0.05$.

4.3. Results

Published data were available to compute nicotine flux for approximately 90 products, spanning the categories of cigarettes, cigarillos, small cigars, waterpipes, ENDS, heated tobacco products, patches, and nicotine gum. Table 8 lists the results obtained for tobacco products that were machine smoked by mimicking human puffing patterns or by standard machine smoking regimens (e.g., Canadian Intense, ISO). The nicotine flux across products ranged four orders of magnitude, from less than 0.1 $\mu\text{g/s}$ to more than 100 $\mu\text{g/s}$, with the low end of the spectrum populated exclusively by nicotine patch and gum products and very low nicotine cigarettes and products above 100 $\mu\text{g/s}$ consisting exclusively of conventional combustible cigarettes. The results are summarized in Table 9.

| Tobacco Product | Brand | Puff Number | Puff duration (s) | Nicotine Yield (mg/unit) | Nicotine Flux ($\mu\text{g/s}$) | Reference | Year of Publication |
|---------------------------------|---|---|--------------------------|---------------------------------|---|------------------|----------------------------|
| Cigarettes | Maintained nicotine cigarette | 15 | 2 | 2.7 | 90.0 | 93 | 1988 |
| | Middle tar cigarette | 15 | 2 | 2.9 | 96.7 | | |
| | Low tar cigarette | 14 | 2.5 | 1.8 | 51.4 | | |
| | Regular-yield brands (9-15 mg ISO tar) | 11.5 | 1.4 | 2 | 124.2 | 94 | 2006 |
| | Matinee extra mild (4 mg ISO tar) | 13.4 | 1.6 | 1.5 | 70.0 | | |
| | Own brand (female smokers) | 13.5 | 1.33 | 1.92 | 106.9 | 95 | 2007 |
| | Own brand (male smokers) | 12 | 1.48 | 2.2 | 123.9 | | |
| | Kent (non-menthol cigarette) | 14.4 | 1.17 | 0.9 | 53.4 | 96 | 2017 |
| | Benson & Hedges Light (menthol cigarette) | 15.1 | 1.23 | 1.05 | 56.5 | | |
| | Marlboro red | 12.2 | 1.68 | 2.54 | 123.9 | | |
| | Lucky Strike | 10.7 | 1.8 | 1.3 | 67.5 | 98 | 2018 |
| | Lucky Strike Menthol | 10 | 2 | 1.3 | 65.0 | | |
| | Lucky Strike | 16.6 | 1.6 | 1.5 | 56.5 | 99 | 2020 |
| | Low-yield cigarettes (≤ 0.8 mg of nicotine/cigarette) | 12.7 | 1.5 | 1.7 | 89.2 | 88 | 2000 |
| | Medium-yield cigarettes (0.9–1.2 mg of nicotine/cigarette) | 12.1 | 1.5 | 2.39 | 131.7 | | |
| | 2R4F | 9.5 | 2 | 0.829 | 43.6 | 100 | 2014 |
| | 1R6F | 8.0 | 2 | 0.73 | 45.6 | 101 | 2018 |
| | 1R6F | 8.4 | 2 | 2.34 | 139.3 | | |
| | 3R4F | 9.0 | 2 | 0.74 | 41.1 | | |
| | 3R4F | 10.7 | 2 | 2.38 | 111.2 | | |
| | Regular-yield brands (9-15 mg ISO tar) | 9 | 2 | 1.1 | 61.1 | 94 | 2006 |
| | | 12.1 | 2 | 2.4 | 99.2 | | |
| | Low-yield cigarettes (≤ 0.8 mg of nicotine/cigarette) | 9 | 2 | 0.7 | 38.9 | 88 | 2000 |
| | Medium-yield cigarettes (0.9–1.2 mg of nicotine/cigarette) | 9 | 2 | 1.11 | 61.7 | | |
| | Marlboro Ultra Smooth | 7.2 | 2 | 0.42 | 29.2 | 102 | 2006 |
| | | 6.9 | 2 | 1.09 | 79.0 | | |
| | Marlboro Regular | 12 | 2 | 1.99 | 82.9 | 103 | 2018 |
| VLNC | VLN King | 9* | 2 | 0.03 | 1.7 | 104 | 2019 |
| Roll Your Own Cigarettes | Average of 13 brands | 12.4 | 2 | 1.3 | 52.4 | 105 | 1985 |
| | Average of 11 brands | 9.42 | 2 | 1.90 | 100.8 | 106 | 2014 |
| | Average of 517 cigarettes made by 26 regular users | 12.3 | 2 | 1.30 | 52.8 | 107 | 1998 |
| Tobacco Heating Products | glo with Bright Tobacco Kent Neostiks | 11.6 | 1.8 | 0.3 | 14.4 | 98 | 2018 |
| | glo with mentholated Intensely Fresh Kent Neostiks | 10 | 1.8 | 0.3 | 16.7 | | |
| | iQOS with Essence tobacco HeatStick | 10.55 | 1.8 | 0.9 | 47.4 | | |
| | glo with Bright Tobacco Kent Neostiks | 15.4 | 1.6 | 0.34 | 13.8 | 99 | 2020 |
| | iQOS with Essence tobacco HeatStick | 15 | 1.4 | 0.98 | 46.7 | | |
| | carbon-based Eclipse | 25 | 2 | 2.36 | 47.2 | 108 | 2019 |
| | Glo with Bright Tobacco Kent Neostiks | 8 | 2 | 0.462 | 28.9 | 109 | 2018 |
| | Glo with mentholated Intensely Fresh Kent Neostiks | 8 | 2 | 0.365 | 22.8 | | |
| | Unspecified Heat not Burn Device | 12 | 2 | 1.4 | 58.3 | | |
| | Unspecified Heat not Burn Device with Mentholated flavor | 12 | 2 | 1.38 | 57.5 | 103 | 2018 |
| | Unspecified Heat not Burn Device | 12 | 4 | 1.41 | 29.4 | | |
| | Unspecified Heat not Burn Device with Mentholated flavor | 12 | 4 | 1.43 | 29.8 | 108 | 2019 |
| | Carbon-based Eclipse | 12 | 2 | 0.14 | 5.8 | | |
| | Carbon-based Eclipse | 18.3 | 2 | 0.56 | 15.3 | | |
| | | Volish, eGo-3 (nicotine concentration 18 mg/ml; liquid composition: Propylene glycol, | 15 | 2.8 | 1.06 | 25.2 | 110 |

| | | | | | | | |
|---|---|------|------|------|------|-----|------|
| Electronic Nicotine Delivery Systems | <i>nicotine, vanillin, linalool, flavorings)</i> | | | | | | |
| | <i>Volish, eGo-3 (nicotine concentration 18 mg/ml; liquid composition: Propylene glycol, glycerin, nicotine, ethanol, flavorings)</i> | 15 | 2.8 | 1.15 | 27.4 | | |
| | <i>Volish, eGo-3 (nicotine concentration 24 mg/ml; liquid composition: Glycerin, nicotine, propylene glycol, linalool, vanillin, flavorings)</i> | 15 | 2.8 | 1.05 | 25.0 | | |
| | <i>Volish, eGo-3 (nicotine concentration 22 mg/ml; liquid composition: Glycerin, propylene glycol, nicotine, flavorings)</i> | 15 | 2.8 | 1.43 | 34.0 | | |
| | <i>Volish, eGo-3 (nicotine concentration 12 mg/ml; liquid composition: Glycerin, propylene glycol, nicotine, flavorings)</i> | 15 | 2.8 | 0.88 | 21.0 | | |
| | <i>Volish, eGo-3 (nicotine concentration 16 mg/ml; liquid composition: Glycerin, propylene glycol, nicotine, flavorings)</i> | 15 | 2.8 | 1.02 | 24.3 | | |
| | <i>Volish, eGo-3 (nicotine concentration 25 mg/ml; liquid composition: Glycerin, propylene glycol, nicotine, ethanol, flavorings)</i> | 15 | 2.8 | 1.36 | 32.4 | | |
| | <i>Volish, eGo-3 (nicotine concentration 28 mg/ml; liquid composition: Glycerin, propylene glycol, nicotine, ethanol, malic acid, flavorings)</i> | 15 | 2.8 | 1.49 | 35.5 | | |
| | <i>Volish, eGo-3 (nicotine concentration 11 mg/ml; liquid composition: Glycerin, nicotine, menthol, vanillin, aromatic oils, vanilla)</i> | 15 | 2.8 | 0.77 | 18.3 | | |
| | <i>Blu Cigs (Tobacco-flavored cartomizers with nicotine concentration of 16 mg/ml)</i> | 33 | 2.75 | 1.2 | 13.2 | 111 | 2015 |
| | <i>V2 Cigs (Tobacco-flavored cartomizers with nicotine concentration of 18 mg/ml)</i> | 31 | 2.54 | 1.4 | 17.8 | | |
| | <i>Lab Assembled ECIG 6 W (E-liquid concentration range 6-18 mg/ml)</i> | 57 | 4.6 | 3.5 | 13.3 | 112 | 2018 |
| | <i>Lab Assembled ECIG 10 W (E-liquid concentration range 6-18 mg/ml)</i> | 46 | 3.8 | 4.2 | 24.0 | | |
| | <i>KangerTech Mini ProTank with own flavor (E-liquid nicotine concentration range 1.6-16.7 mg/ml and PG/VG ratio range of 69/31-5/95)</i> | 106 | 4.3 | 3.4 | 7.5 | 113 | 2018 |
| | <i>KangerTech Mini ProTank with strawberry flavored e-liquid (E-liquid nicotine concentration 19.9 mg/ml and PG/VG ratio of 40/60)</i> | 73 | 3.2 | 5.4 | 23.1 | | |
| | <i>KangerTech Mini ProTank with Tobacco flavored e-liquid (E-liquid nicotine concentration 19.3 mg/ml and PG/VG ratio of 44/56)</i> | 69 | 2.8 | 4.1 | 21.2 | | |
| | <i>Vype with 'Twilight Tobacco' flavored e-liquid (E-liquid nicotine concentration 5 mg/ml and PG/VG ratio of 40/60)</i> | 61.1 | 1.45 | 0.75 | 8.5 | 99 | 2020 |
| | <i>Vapour 2 cigs (E-liquid nicotine concentration 20 mg/ml and PG/VG ratio of 50/50)</i> | 12 | 2 | 0.46 | 19.2 | 103 | 2018 |
| | | 12 | 4 | 0.86 | 17.9 | | |

| | | | | | | | |
|--|---|-------------------------|------|-------|-------|------|------|
| | eGo style, Epsilon (E-liquid nicotine concentration 20 mg/ml and PG/VG ratio of 50/50) | 12 | 2 | 0.51 | 21.3 | | |
| | | 12 | 4 | 1.73 | 36.0 | | |
| | EVIC VTC Mini battery with Nautilus Mini atomizer (E-liquid nicotine concentration 20 mg/ml and PG/VG ratio of 50/50) | 12 | 2 | 0.82 | 34.2 | | |
| | | 12 | 4 | 1.84 | 38.3 | | |
| Electronic Nicotine Delivery Systems | Vype Disposable Regular | 1 | 3 | 0.04 | 13.3 | 108 | 2019 |
| | | 1 | 5 | 0.06 | 12.0 | | |
| | Intellicig XL | 1 | 3 | 0.03 | 10.0 | | |
| | | 1 | 5 | 0.07 | 14.0 | | |
| | V4L CoolCart cartomizers (8.53 mg/ml nicotine concentration) | 2 | 15 | 0.11 | 3.7 | 77 | 2015 |
| | | 4 | 15 | 0.30 | 5.0 | | |
| | | 4 | 15 | 0.29 | 4.8 | | |
| | | 8 | 15 | 0.72 | 6.0 | | |
| | | 8 | 15 | 0.68 | 5.7 | | |
| | | 2 | 15 | 0.64 | 21.3 | | |
| | | 4 | 15 | 1.18 | 19.7 | | |
| | | 4 | 15 | 1.50 | 25.0 | | |
| | | 8 | 15 | 3.23 | 26.9 | | |
| | | 8 | 15 | 3.09 | 25.8 | | |
| | V4L CoolCart cartomizers (15.73 mg/ml nicotine concentration) | 4 | 15 | 0.48 | 8.0 | 77 | 2015 |
| | | 8 | 15 | 4.7 | 39.2 | | |
| | JUUL US - Tobacco flavor (65 mg/ml nicotine concentration) | 15 | 4 | 1.3 | 21.7 | 114 | 2020 |
| | JUUL UK - Tobacco flavor (19 mg/ml nicotine concentration) | 15 | 4 | 0.4 | 6.7 | | |
| | JUUL US - Tobacco flavor (69 mg/ml nicotine concentration) | 15 | 4 | 2.07 | 34.5 | 115 | 2019 |
| | JUUL US - Tobacco flavor | 1 | 2.5 | 0.157 | 62.8 | 116 | 2019 |
| | JUUL US – Crème brulee flavor | 1 | 2.5 | 0.170 | 68.0 | | |
| | JUUL US – Fruit punch flavor | 1 | 2.5 | 0.154 | 61.6 | | |
| | JUUL US - Mint flavor | 1 | 2.5 | 0.188 | 75.2 | | |
| | JUUL US – Tobacco flavor (69.8 mg/ml nicotine concentration) | 15 | 4 | 1.67 | 27.8 | 117 | 2021 |
| | Ezzy Oval – Berry Cool flavor (53.8 mg/m nicotine concentration) | 15 | 4 | 4.07 | 67.8 | | |
| | Ezzy Oval – Mango Lychee flavor (75.4 mg/m nicotine concentration) | 15 | 4 | 5.44 | 90.7 | | |
| | Hyde – Cherry lemonade flavor (86.9 mg/m nicotine concentration) | 15 | 4 | 3.15 | 52.5 | | |
| | Puff Bar – Banana ice flavor (83.4 mg/m nicotine concentration) | 15 | 4 | 6.72 | 112.0 | | |
| SEA – Mint flavor (54.3 mg/m nicotine concentration) | 15 | 4 | 1.67 | 27.8 | | | |
| - | 77.7 | 3.6 | 1.6 | 5.8 | 118 | | |
| Waterpipes | - | 290 | 2.9 | 5 | 5.9 | 51 | 2018 |
| | - | 220 | 2.8 | 4.8 | 7.8 | 119 | 2010 |
| | - | 105 | 2.6 | 5.4 | 19.8 | 54 | 2019 |
| | - | 171 | 2.6 | 2.96 | 6.7 | 46 | 2005 |
| | - | 100 | 3.0 | 2.25 | 7.5 | 73 | 2003 |
| | - | 171 | 2.6 | 6.06 | 13.6 | 49 | 2008 |
| | - | 171 | 2.6 | 7.75 | 17.4 | 67 | 2011 |
| | Cigarillos | <i>Black & Mild</i> | 23.1 | 2.8 | 2.3 | 35.6 | 120 |
| <i>Winchester</i> | | 9.8 | 2 | 1.8 | 91.8 | 120 | 2018 |
| Small Cigars | Average values of 8 commercially available small cigars in the US | 16.6 | 2 | 1.24 | 37.3 | 101 | 2018 |
| | | 16.5 | 2 | 3.49 | 105.8 | | |
| | Little cigars with cigar wrapper (average of 5 brands) | 8.5 | 2 | 1.60 | 94.1 | 121 | 1976 |
| | Little cigars with paper wrapper (average of 5 brands) | 9.4 | 2 | 1.60 | 85.1 | | |
| | Average of 10 brands | 14.4 | 2 | 2.1 | 72.9 | 105 | 1985 |
| Large Cigars | Average of 5 brands | 70.3 | 1.5 | 2.4 | 22.8 | 121 | 1976 |
| | Average of 6 brands | 108 | 1.5 | 1.9 | 11.7 | 105 | 1985 |
| Kretek | Sampoerna | 12.6 | 2 | 0.74 | 29.4 | 100 | 2014 |
| | Garam | 17.3 | 2 | 1.78 | 51.4 | | |

| | | | | | | | |
|-----------------------|----------------------|------|--------|------|------|--------------------|-----------|
| | Kretek-R | 14.4 | 2 | 1.72 | 59.7 | | |
| Bidi | Average of 21 brands | 21 | 2 | 2.70 | 64.3 | ¹²² | 2003 |
| | Average of 24 brands | 17 | 2 | 1.86 | 54.7 | ¹²³ | 1998 |
| Nicotine Patch | NiQuitin Clear 7 mg | - | 24 hrs | 7 | 0.08 | ¹²⁴ | 2019 |
| | NiQuitin Clear 14 mg | | 24 hrs | 14 | 0.16 | | |
| | NiQuitin Clear 21 mg | | 24 hrs | 21 | 0.24 | | |
| Nicotine Gum | Zonnic 2mg | - | 30 min | 2 | 1.11 | ^{125,126} | 2018/2019 |

Table 8: Summary of the nicotine yield and flux of various tobacco products and the corresponding puffing topography parameters. * Average puff number under ISO smoking regime was used.

| Product | N | Year span | Flux ($\mu\text{g/s}$) | |
|---------------------------------|----|-----------|--------------------------|----------|
| | | | Mean (SD) | Range |
| Combustible cigarettes | 27 | 1988-2020 | 79(32) | 29-140 |
| ENDS | 52 | 2015-2021 | 29(23) | 3.7-110 |
| Heated tobacco products | 14 | 2018-2020 | 31(18) | 5.8-58 |
| Waterpipe | 8 | 2003-2019 | 11(5.6) | 5.8-20 |
| Cigars/cigarillos | 9 | 1976-2018 | 62(35) | 12-110 |
| Roll your own | 3 | 1985-2014 | 69(28) | 52-100 |
| Bidi | 2 | 1988-2003 | 60(6.8) | 55-64 |
| Kretek | 3 | 2014 | 47(16) | 29-60 |
| Nicotine patch and gum products | 4 | 2018-2019 | 0.4(0.48) | 0.08-1.1 |
| Very low nicotine cigarettes | 1 | 2019 | 1.7(-) | - |

Table 9: Computed nicotine flux by tobacco product category. N indicates the number of products reported, while year span indicates years of publication for the studies included. SD = standard deviation.

We also found a significant increase in reported flux over time (Figure 12) for ENDS products ($4.5 \mu\text{g/s/year}$; $p < 0.001$). Whereas prior to 2018, no publications reported products with a flux exceeding $40 \mu\text{g/s}$, from 2019 onwards, nearly 40% of the tested products exceeded a flux of $60 \mu\text{g/s}$. The upper quartile flux for ENDS products in a given year also increased significantly at a mean rate of $9.5 \mu\text{g/s/year}$ ($p < 0.001$).

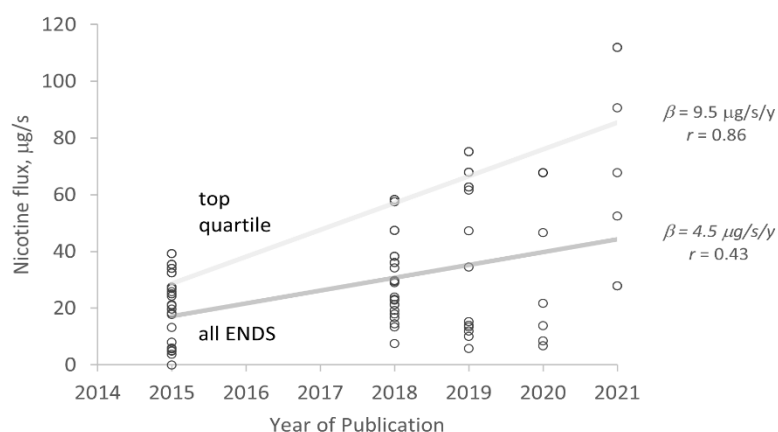


Figure 12: Reported nicotine flux of ENDS products by year of manuscript publication. ($p < 0.001$ for both regression lines)

4.4. Discussion

Nicotine flux is a performance metric that describes the acute nicotine throughput of a tobacco product, the net outcome of the interactions between numerous product design and operating variables. While nicotine flux represents the rate at which nicotine can enter the human body, and therefore the theoretical limit of the rate of delivery to the brain, the rate is mediated by other factors that influence the pharmacokinetics of nicotine delivery. For inhaled products, these factors include such things as the particle size distribution and freebase-to-protonated nicotine ratio of the aerosol. In this study, we sought to document nicotine flux from a range of tobacco products whose yields and puffing parameters had been reported in the literature. One limitation of this study is that products studied by previous researchers may not represent well the sales-weighted average of each category. A second limitation is that reported smoking machine studies may not have always used representative puffing parameters (e.g., puff velocity, duration, or interpuff interval), biasing nicotine yield, and, therefore, the computed flux. The most accurate analytical determinations of nicotine emissions are made using puffing conditions appropriate to the product in

question; for example, users of large sub-Ohm ENDS devices typically draw up to an order of magnitude greater flow rate than a user of a small pod-based device.

We found that for inhalable tobacco products, combustible cigarettes exhibited the greatest average nicotine flux, while waterpipes exhibited the greatest nicotine yield per session. Overall, nicotine patches had the greatest yields but also, owing to the long duration of use per unit, the lowest fluxes. These findings underscore the limitations of nicotine yield as a regulatory construct for tobacco products that vary widely; in these cases, greater yield was associated with *lower* abuse liability.

We also found significant variability in flux within and across product categories, as illustrated in Figure 13. While ENDS generally exhibited nicotine fluxes lower than those of combustible cigarettes, reports from 2018 onwards began revealing ENDS products whose fluxes were equivalent to combustible cigarettes. Importantly, the 110 $\mu\text{g/s}$ maximum flux reported to date for an ENDS product does not represent an intrinsic physical limit. With products available over the counter today, an ENDS user can readily access a liquid/device combination whose flux exceeds any value yet reported. For example, based on the mathematical model of Talih et al.¹²⁷, a device operating at 60 W with an EU-compliant 20 mg/ml nicotine concentration liquid can produce a flux of approximately 240 $\mu\text{g/s}$, roughly double the maximum reported for any combustible cigarette.

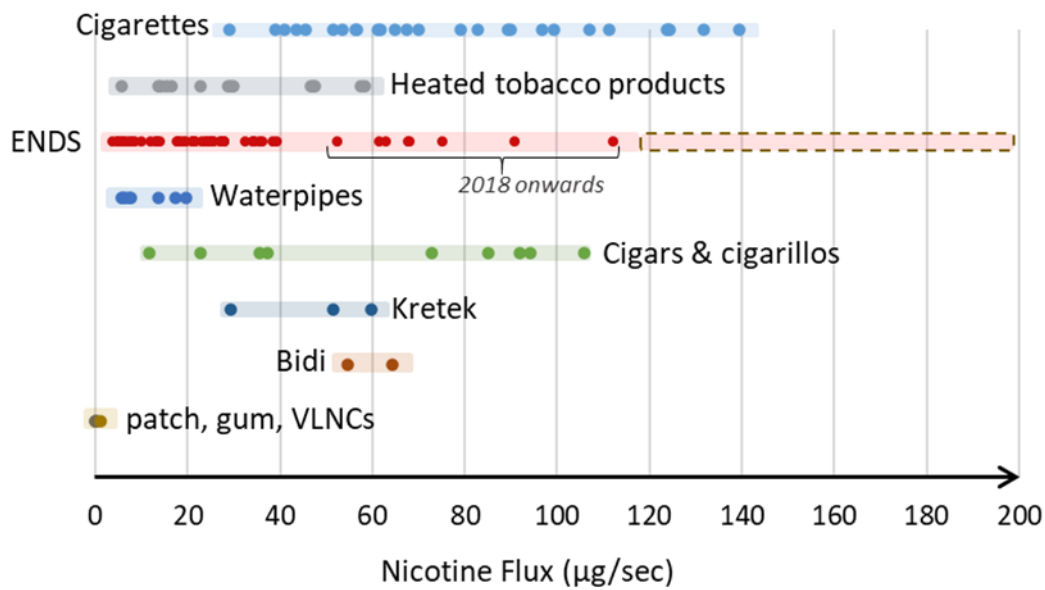


Figure 13: Nicotine flux ranges across tobacco products. The dashed line for ENDS represents the capacity of current over-the-counter products to exceed values reported to date.

The current regulatory environment therefore allows marketing ENDS products whose nicotine emission rate exceeds that of the high abuse liability combustible cigarette. Combined with emerging evidence that the convenience of ENDS use leads to far more frequent nicotine administration throughout the day than for combustible cigarettes^{128,129}, the availability of high-flux ENDS products may portend greater population-wide nicotine dependence than was present prior to the advent of ENDS, if this outcome has not already been realized. Empirical data on the relationship between flux, acute delivery, and dependence is too thin to evaluate this hypothesis at present; such data is urgently needed. Of note, Do et al.¹³⁰ recently reported an association between nicotine flux and dependence scores in a pilot study of experienced users of pod-based devices.

Given the approximate doubling of ENDS nicotine flux from 2015 to 2020, policy makers may not have the leeway to wait for a definitive evidence base to emerge, and

may find it prudent to regulate flux in the interim. There is little reason to suspect that exceeding the nicotine flux of combustible cigarettes is necessary to improve public health. With this starting point, an upper limit on ENDS nicotine flux could be, at most, 140 µg/. However, given the greater convenience and greater use frequency observed in ENDS users, this upper limit, if applied to ENDS, may still lead to greater population-level nicotine dependence. For this reason, one potential approach is to use the mean observed for combustible cigarette flux (i.e., approximately 80 mg/sec, see Table 9) as a temporary ceiling for over-the-counter ENDS products, with further adjustments informed by empirical investigations aimed at understanding the abuse liability of ENDS products across populations of particular interest (e.g., nicotine naïve individuals, former smokers at risk for relapse). Of course, if empirical work demonstrates that higher flux ENDS are safe and effective for smoking cessation, these products can be made available to cigarette smokers in a manner that does not risk the health of nicotine-naïve individuals (e.g., restricted access rather than over-the-counter availability). An additional concern is that ENDS aerosols contain varying concentrations of toxicants such as carbonyl species. Thus, minimizing the amount of inhaled aerosol may be desirable because it can reduce user exposure to harmful toxicants. From this perspective, to the extent that a user seeks to attain a given nicotine intake, too low a nicotine flux can, perversely, increase non-nicotine toxicant exposure because it may drive more prolonged puffing bouts.

Policymakers interested in reducing nicotine dependence at the population level would do well to address nicotine flux as a regulatory target and avoid the mistake of using inappropriate proxies (e.g., liquid nicotine concentration) that cannot, by themselves, be used to control the nicotine dose inhaled by ENDS users.

APPENDIX

ENDS model description

The temperature and liquid vaporization rate, \dot{m}_{v_0} emitted by the ENDS during a puff were determined using a numerical simulation previously described by Talih et al.¹²⁷ The model is based on unsteady energy and mass balances and equilibrium ideal solution thermodynamics applied to a single-zone control volume bounding the heating coil and wick of the ENDS device.

In brief, the temperature of the ENDS heating coil and wick is computed at a time step of 0.1 milliseconds during and between puffs, accounting for the electrical power delivered by the device, the heating and subsequent vaporization of fresh liquid into the heated zone, and the various losses due to conduction and convection from the heated zone. The model accounts for liquid composition changes during evaporation and boiling, depending on the instantaneous temperature in the heated zone.

To account for thermal energy and condensation losses from the aerosol as it travels downstream of the vaporization zone through the mouthpiece, we coupled to the model of Talih et al. (2017)¹²⁷ to a boundary-layer heat transfer model using the geometry of the Subox Mini-C ENDS product used in the clinical studies, as illustrated in Figure A1. At each time step, the adiabatic mixing temperature T_1 between the hot vapors and the air flowing over the coil/wick assembly is computed. The mixture then loses heat by convection to the walls of the ENDS mouthpiece tube. The average heat transfer coefficient \bar{h} through the tube length is calculated based on the flow rate of the inhaled aerosol and tube dimensions so that the temperature T_2 of the inhaled aerosol could be determined by²⁹:

$$T_2 = T_{tube} - \exp\left(-\frac{Per L}{\dot{m} c_p} \bar{h}\right)(T_{tube} - T_1) \quad (A1)$$

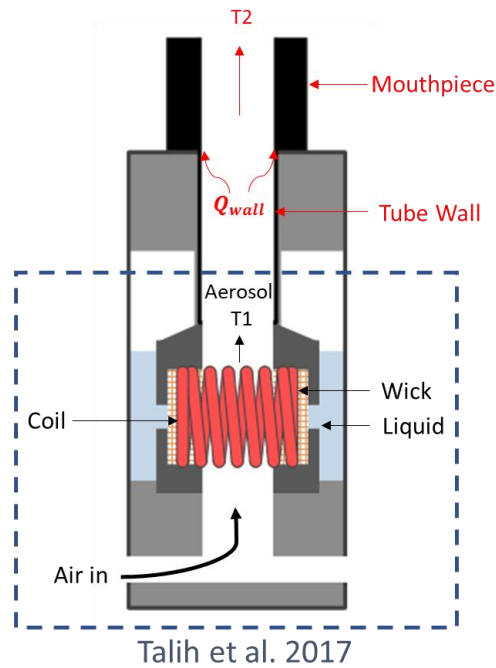


Figure A1: Inhalation temperature at the device mouthpiece computed by combining the model of Talih et al. (2017) and thermal energy losses to the tube walls.

To verify the simulation of the ENDS/mouthpiece operation during a puff, the aerosol temperature exiting the mouthpiece was measured by a thermocouple installed at the mouthpiece exit while the device was puffed using the AUB Aerosol Lab Vaping Instrument (ALVIN). The thermocouple data was acquired at 4 Hz using a National Instruments-based data acquisition system.

Measurements were made under 18 different conditions. These included varying liquid PG/ VG ratio (70/30 vs 30/70), three flow rates (4,10, and 15 lpm), and three ENDS power settings (13.5, 30, and 40.5 W). For each condition, ALVIN was programmed to generate 10 puffs of 4 second duration with an inter-puff interval of 10 seconds. The same test conditions were run using the model and compared to

experimental results. Model predicted temperatures showed significant correlation with those measured experimentally as shown in Figure A2.

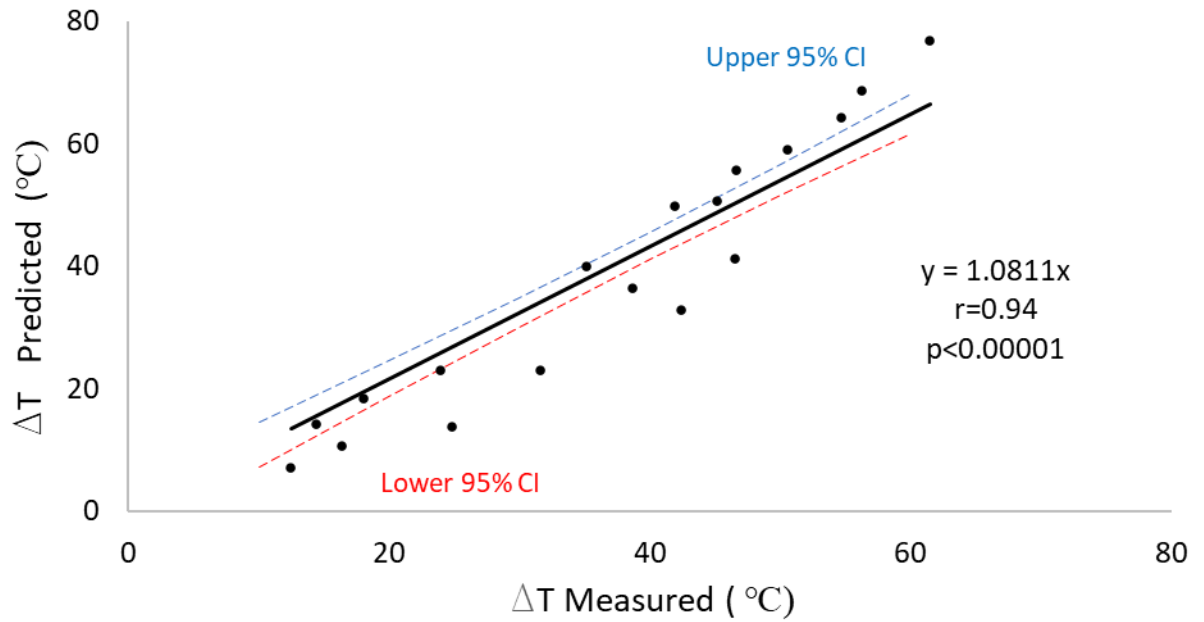


Figure A2: Model predicted versus measured aerosol temperature difference between the outlet of the ENDS mouthpiece and the ambient. Each point represents the mean temperature of 10 puffs drawn at each condition

Upper airway cross-sectional area and perimeter variations

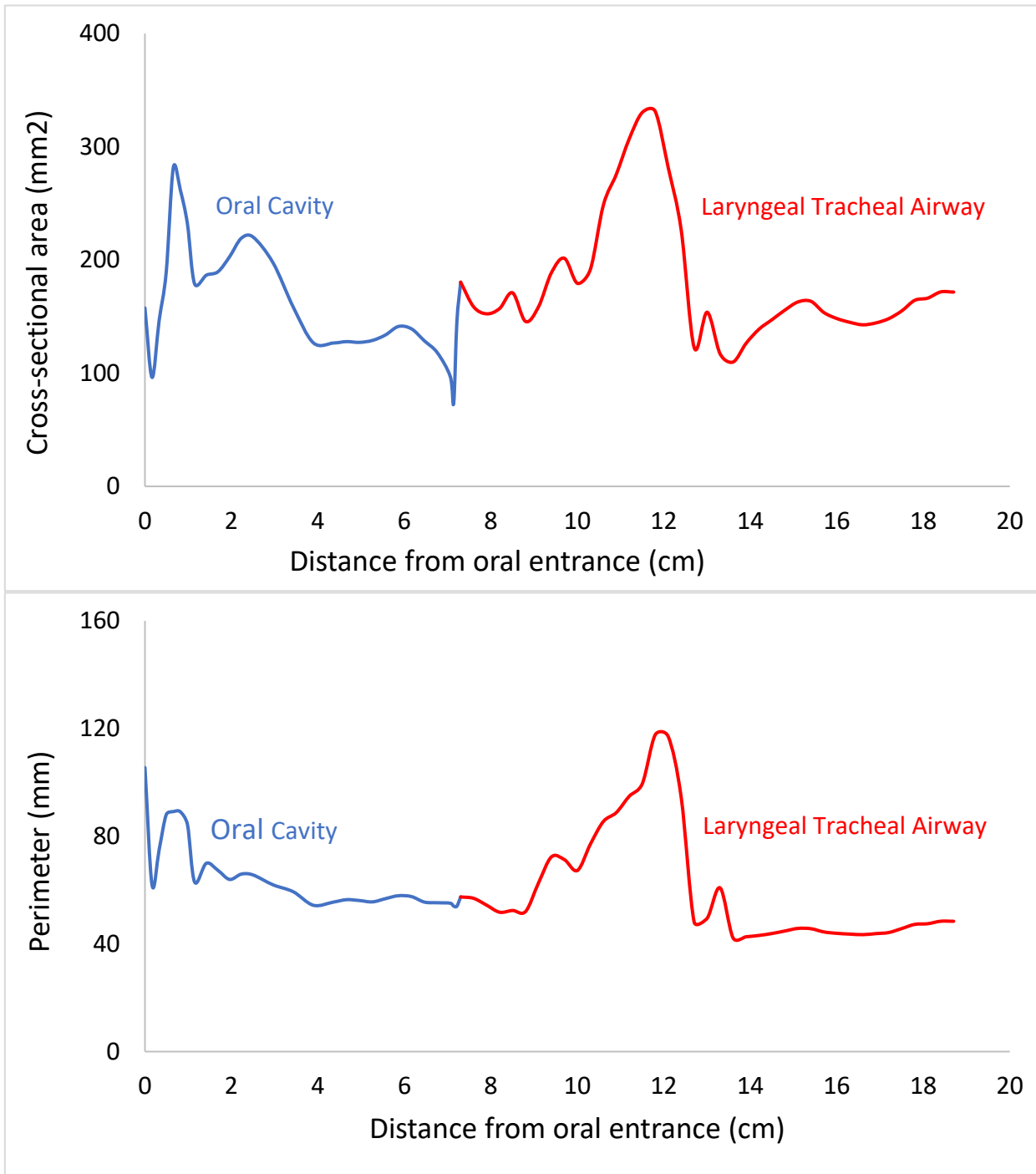


Figure A3: Cross-sectional area and perimeter variations along the upper airway

Upper airway Nusselt number values

| <i>Airway Segment</i> | <i>Flow rate (LPM)</i> | | | | | | | | | | | | | | | | | | | |
|-----------------------|------------------------|----------|----------|----------|----------|----------|----------|----------|----------|-----------|-----------|-----------|-----------|-----------|-----------|-----------|-----------|-----------|-----------|-----------|
| | 1 | 2 | 3 | 4 | 5 | 6 | 7 | 8 | 9 | 10 | 11 | 12 | 13 | 14 | 15 | 16 | 17 | 18 | 19 | 20 |
| 1 | 9.8 | 13.2 | 15.8 | 18.0 | 19.9 | 21.7 | 23.4 | 25.0 | 26.5 | 28.0 | 29.4 | 32.0 | 32.1 | 33.3 | 34.6 | 35.8 | 37.0 | 38.1 | 39.3 | 42.5 |
| 2 | 7.9 | 9.3 | 10.5 | 11.8 | 13.2 | 14.6 | 16.1 | 17.6 | 19.1 | 20.7 | 22.2 | 24.2 | 25.4 | 27.0 | 28.7 | 30.3 | 31.9 | 33.6 | 35.2 | 36.3 |
| 3 | 8.8 | 9.8 | 10.7 | 11.7 | 12.7 | 13.8 | 15.0 | 16.2 | 17.4 | 18.6 | 19.8 | 21.6 | 22.0 | 23.1 | 24.1 | 25.0 | 25.9 | 26.8 | 27.7 | 29.3 |
| 4 | 10.5 | 12.6 | 15.3 | 18.4 | 21.9 | 25.3 | 28.8 | 32.2 | 35.7 | 39.1 | 42.6 | 46.4 | 49.6 | 53.0 | 56.2 | 59.2 | 62.2 | 65.3 | 68.3 | 72.3 |
| 5 | 6.2 | 7.3 | 9.2 | 11.8 | 15.1 | 18.6 | 22.1 | 25.8 | 29.4 | 32.8 | 36.0 | 39.3 | 11.4 | 44.3 | 47.3 | 50.5 | 53.6 | 56.9 | 60.1 | 60.0 |
| 6 | 6.9 | 5.6 | 4.0 | 3.7 | 3.7 | 3.7 | 3.7 | 3.7 | 3.7 | 3.7 | 3.7 | 3.7 | 19.8 | 3.7 | 3.7 | 3.7 | 3.7 | 3.7 | 3.7 | 3.7 |
| 7 | 5.6 | 6.3 | 6.4 | 5.9 | 4.7 | 3.7 | 3.7 | 3.7 | 3.7 | 3.7 | 3.7 | 3.7 | 3.7 | 3.7 | 3.7 | 3.7 | 3.7 | 3.7 | 3.7 | 3.7 |
| 8 | 4.2 | 4.5 | 4.4 | 4.0 | 3.7 | 3.7 | 3.7 | 3.7 | 3.7 | 3.7 | 3.7 | 3.7 | 3.7 | 3.7 | 3.7 | 3.7 | 3.7 | 3.7 | 3.7 | 3.7 |
| 9 | 3.7 | 3.9 | 4.2 | 4.4 | 4.7 | 4.9 | 5.0 | 6.0 | 3.7 | 3.7 | 3.7 | 3.7 | 3.7 | 3.7 | 3.7 | 3.7 | 3.7 | 3.7 | 3.7 | 3.7 |
| 10 | 3.7 | 3.7 | 3.9 | 4.0 | 4.1 | 4.2 | 4.3 | 3.7 | 4.6 | 4.8 | 5.1 | 5.6 | 5.7 | 3.7 | 3.7 | 3.7 | 3.7 | 3.7 | 3.7 | 3.7 |
| 11 | 3.8 | 4.2 | 4.6 | 5.2 | 6.0 | 7.3 | 9.2 | 11.6 | 14.0 | 16.0 | 17.7 | 19.4 | 21.3 | 23.3 | 25.1 | 26.4 | 27.3 | 28.0 | 28.7 | 31.8 |
| 12 | 3.8 | 4.5 | 5.4 | 6.3 | 7.5 | 9.0 | 10.2 | 10.7 | 10.8 | 11.0 | 11.9 | 12.9 | 15.2 | 14.9 | 14.0 | 13.7 | 14.4 | 15.8 | 17.1 | 17.9 |
| 13 | 3.7 | 3.7 | 4.4 | 5.3 | 6.1 | 6.7 | 7.0 | 7.2 | 7.1 | 6.9 | 6.6 | 7.2 | 5.2 | 4.8 | 5.1 | 5.6 | 5.9 | 6.0 | 6.0 | 6.0 |
| 14 | 3.7 | 5.2 | 6.8 | 8.3 | 9.6 | 10.4 | 10.9 | 11.2 | 11.6 | 12.1 | 12.6 | 13.7 | 13.7 | 14.6 | 15.3 | 15.9 | 16.4 | 16.9 | 17.4 | 18.8 |
| 15 | 3.7 | 5.3 | 6.9 | 8.5 | 10.1 | 11.6 | 12.8 | 14.0 | 14.8 | 15.4 | 16.0 | 17.4 | 17.2 | 17.8 | 18.5 | 19.3 | 20.0 | 20.7 | 21.4 | 23.5 |
| 16 | 4.1 | 5.8 | 7.5 | 9.1 | 10.5 | 11.8 | 13.0 | 14.1 | 15.0 | 15.6 | 16.3 | 17.7 | 17.5 | 18.2 | 18.8 | 19.5 | 20.3 | 21.0 | 21.6 | 23.7 |
| 17 | 3.7 | 4.5 | 5.9 | 7.3 | 8.4 | 9.4 | 10.3 | 11.1 | 11.7 | 12.2 | 12.7 | 13.8 | 13.5 | 13.9 | 14.4 | 14.9 | 15.4 | 15.9 | 16.4 | 18.0 |
| 18 | 3.7 | 4.5 | 5.8 | 7.1 | 8.2 | 9.2 | 10.1 | 10.9 | 11.6 | 12.2 | 12.8 | 14.0 | 13.8 | 14.2 | 14.7 | 15.2 | 15.7 | 16.2 | 16.7 | 18.4 |
| 19 | 3.7 | 4.7 | 6.0 | 7.3 | 8.3 | 9.1 | 9.9 | 10.6 | 11.3 | 11.9 | 12.5 | 13.6 | 13.5 | 14.0 | 14.4 | 14.9 | 15.4 | 15.9 | 16.4 | 18.0 |
| 20 | 6.9 | 9.0 | 11.3 | 13.3 | 15.0 | 16.4 | 17.7 | 18.9 | 20.1 | 21.4 | 22.6 | 24.7 | 24.6 | 25.5 | 26.3 | 27.2 | 28.0 | 28.9 | 29.7 | 32.5 |
| 21 | 3.7 | 3.7 | 3.7 | 3.7 | 3.7 | 3.7 | 3.9 | 4.1 | 4.4 | 4.6 | 4.9 | 5.3 | 5.4 | 5.6 | 5.8 | 6.0 | 6.2 | 6.4 | 6.6 | 6.6 |
| 22 | 3.7 | 3.7 | 3.7 | 3.7 | 3.7 | 3.8 | 4.0 | 4.2 | 4.5 | 4.7 | 5.0 | 5.5 | 5.5 | 5.7 | 5.9 | 6.1 | 6.3 | 6.5 | 6.7 | 6.8 |
| 23 | 3.7 | 4.7 | 5.7 | 6.6 | 7.3 | 7.9 | 8.5 | 9.0 | 9.6 | 10.2 | 10.8 | 11.8 | 11.9 | 12.4 | 12.8 | 13.2 | 13.6 | 13.9 | 14.3 | 15.6 |
| 24 | 4.3 | 5.2 | 6.3 | 7.2 | 8.1 | 8.8 | 9.5 | 10.2 | 10.8 | 11.4 | 12.1 | 13.2 | 13.4 | 14.0 | 14.5 | 15.0 | 15.5 | 16.0 | 16.4 | 17.8 |
| 25 | 5.9 | 6.7 | 7.5 | 8.2 | 8.9 | 9.5 | 10.1 | 10.6 | 11.2 | 11.7 | 12.2 | 13.3 | 13.3 | 13.8 | 14.2 | 14.6 | 15.0 | 15.4 | 15.8 | 16.9 |
| 26 | 12.4 | 15.3 | 17.1 | 18.3 | 19.4 | 20.6 | 21.9 | 23.3 | 24.7 | 26.1 | 27.5 | 30.0 | 30.2 | 31.5 | 32.6 | 33.6 | 34.7 | 35.7 | 36.7 | 39.0 |
| 27 | 14.7 | 21.2 | 28.0 | 34.9 | 43.3 | 51.4 | 59.8 | 68.0 | 72.1 | 78.7 | 85.1 | 92.9 | 99.5 | 106.3 | 113.4 | 120.5 | 127.6 | 136.6 | 144.1 | 149.9 |
| 28 | 19.4 | 26.2 | 32.0 | 35.3 | 39.4 | 43.6 | 46.9 | 50.0 | 55.0 | 64.8 | 78.0 | 85.1 | 100.2 | 110.1 | 117.5 | 124.2 | 129.8 | 125.9 | 134.5 | 144.1 |

Table A10: Nusselt number values in the oral cavity “OC” at flow rates ranging between 1 and 20 liters/minute

| Airway Segment | Flow rate (LPM) | | | | | | | | | | | | | | | | | | | |
|----------------|-----------------|-----|------|------|------|------|------|------|------|------|------|------|------|------|------|------|------|------|------|------|
| | 1 | 2 | 3 | 4 | 5 | 6 | 7 | 8 | 9 | 10 | 11 | 12 | 13 | 14 | 15 | 16 | 17 | 18 | 19 | 20 |
| 29 | 4.5 | 4.0 | 3.8 | 4.1 | 3.7 | 3.7 | 3.7 | 3.7 | 5.6 | 5.8 | 5.0 | 5.5 | 3.7 | 3.7 | 3.7 | 3.7 | 9.1 | 3.7 | 5.4 | 6.0 |
| 30 | 3.8 | 4.7 | 6.2 | 7.1 | 8.5 | 9.4 | 10.9 | 12.8 | 11.6 | 12.6 | 13.5 | 14.7 | 15.5 | 16.6 | 17.8 | 18.2 | 9.0 | 13.7 | 5.3 | 22.3 |
| 31 | 5.0 | 7.6 | 9.3 | 10.3 | 12.7 | 14.0 | 15.2 | 15.4 | 20.1 | 20.2 | 20.0 | 21.8 | 18.8 | 17.5 | 14.7 | 13.5 | 12.5 | 3.7 | 3.7 | 3.7 |
| 32 | 5.7 | 9.8 | 12.8 | 12.9 | 11.5 | 10.8 | 9.3 | 7.3 | 9.7 | 9.6 | 9.8 | 10.7 | 10.8 | 11.7 | 13.7 | 15.4 | 16.7 | 22.1 | 27.2 | 30.3 |
| 33 | 5.3 | 9.0 | 12.3 | 14.2 | 12.0 | 10.2 | 9.1 | 9.5 | 9.1 | 9.6 | 3.7 | 3.7 | 3.7 | 5.1 | 7.2 | 9.0 | 11.0 | 24.3 | 26.6 | 30.0 |
| 34 | 4.4 | 7.4 | 9.7 | 11.1 | 12.2 | 12.9 | 13.6 | 14.3 | 7.4 | 7.9 | 16.6 | 18.1 | 18.9 | 20.2 | 21.6 | 23.1 | 24.7 | 29.6 | 30.5 | 28.2 |
| 35 | 3.7 | 6.0 | 7.9 | 9.3 | 10.6 | 11.6 | 12.5 | 13.3 | 13.8 | 14.4 | 15.3 | 16.7 | 17.9 | 19.3 | 20.6 | 22.0 | 23.3 | 23.9 | 25.3 | 26.1 |
| 36 | 3.7 | 5.4 | 6.9 | 8.1 | 10.0 | 11.2 | 11.9 | 12.4 | 11.2 | 11.4 | 11.9 | 12.9 | 13.2 | 14.2 | 15.5 | 16.7 | 17.8 | 18.8 | 19.8 | 19.7 |
| 37 | 4.1 | 5.8 | 6.8 | 7.9 | 9.1 | 11.2 | 13.3 | 14.8 | 16.5 | 18.0 | 19.1 | 20.8 | 19.8 | 20.4 | 20.9 | 21.3 | 21.8 | 24.8 | 25.9 | 27.6 |
| 38 | 3.7 | 4.9 | 6.2 | 7.2 | 8.4 | 9.6 | 11.0 | 12.4 | 13.3 | 14.8 | 16.3 | 17.8 | 18.0 | 19.1 | 20.2 | 21.3 | 22.5 | 26.8 | 28.7 | 27.7 |
| 39 | 3.7 | 3.7 | 4.5 | 5.8 | 7.9 | 9.8 | 11.3 | 13.1 | 13.6 | 14.9 | 16.2 | 17.7 | 19.3 | 20.6 | 21.9 | 23.6 | 25.5 | 26.3 | 27.5 | 29.1 |
| 40 | 3.7 | 3.7 | 3.7 | 4.4 | 6.3 | 7.6 | 9.2 | 10.7 | 10.9 | 11.6 | 12.6 | 13.8 | 15.5 | 16.7 | 18.1 | 19.2 | 20.2 | 19.5 | 19.7 | 22.4 |
| 41 | 3.7 | 3.7 | 3.8 | 5.1 | 7.4 | 10.5 | 13.3 | 15.6 | 16.5 | 18.3 | 20.1 | 21.9 | 24.4 | 25.4 | 26.5 | 27.8 | 29.1 | 31.0 | 32.3 | 35.1 |
| 42 | 3.7 | 3.7 | 4.4 | 6.3 | 8.9 | 11.0 | 11.8 | 12.1 | 12.9 | 14.5 | 15.7 | 17.2 | 15.9 | 17.0 | 18.0 | 18.8 | 19.7 | 24.0 | 25.7 | 24.9 |
| 43 | 3.7 | 3.7 | 3.7 | 5.6 | 8.5 | 10.5 | 11.3 | 11.5 | 11.5 | 11.9 | 13.2 | 14.4 | 14.6 | 15.3 | 16.2 | 16.9 | 17.6 | 19.5 | 20.5 | 21.2 |
| 44 | 3.7 | 3.7 | 3.7 | 3.7 | 4.0 | 6.1 | 8.0 | 9.1 | 10.1 | 10.2 | 9.6 | 10.5 | 10.0 | 10.4 | 10.6 | 10.9 | 11.1 | 10.3 | 10.5 | 12.9 |
| 45 | 3.7 | 3.7 | 3.7 | 3.7 | 3.7 | 3.7 | 3.7 | 3.7 | 3.7 | 4.1 | 4.2 | 4.5 | 3.7 | 3.7 | 3.7 | 3.7 | 3.7 | 3.7 | 3.7 | 3.7 |
| 46 | 3.7 | 3.7 | 3.7 | 3.7 | 3.7 | 3.7 | 3.7 | 3.7 | 3.7 | 3.7 | 3.9 | 4.3 | 3.7 | 5.9 | 3.7 | 6.1 | 3.7 | 5.0 | 5.0 | 6.0 |
| 47 | 3.7 | 3.8 | 5.0 | 6.3 | 3.7 | 3.7 | 3.7 | 3.7 | 3.8 | 18.3 | 6.7 | 7.3 | 21.9 | 10.2 | 25.2 | 10.5 | 28.9 | 8.5 | 8.4 | 10.0 |
| 48 | 3.7 | 3.7 | 3.8 | 4.2 | 4.9 | 5.8 | 6.7 | 7.7 | 9.1 | 9.9 | 10.4 | 11.3 | 10.4 | 10.7 | 11.2 | 11.8 | 12.4 | 13.3 | 13.9 | 14.7 |
| 49 | 3.7 | 3.7 | 3.7 | 3.7 | 3.9 | 4.4 | 5.0 | 5.5 | 5.8 | 6.4 | 7.0 | 7.6 | 7.8 | 8.1 | 8.3 | 8.5 | 8.6 | 9.3 | 9.6 | 10.1 |
| 50 | 3.7 | 3.7 | 3.9 | 4.6 | 5.9 | 7.3 | 9.1 | 10.8 | 12.5 | 14.3 | 16.1 | 17.5 | 18.5 | 19.8 | 21.3 | 22.9 | 24.6 | 26.1 | 27.9 | 28.7 |
| 51 | 3.7 | 3.7 | 3.7 | 4.6 | 6.1 | 8.2 | 10.5 | 13.3 | 15.3 | 17.6 | 19.8 | 21.6 | 23.3 | 24.5 | 25.3 | 25.9 | 26.3 | 25.8 | 25.8 | 31.6 |
| 52 | 3.7 | 3.7 | 3.7 | 3.7 | 4.1 | 5.3 | 6.6 | 7.7 | 8.3 | 8.9 | 8.7 | 9.5 | 7.9 | 7.5 | 7.1 | 6.8 | 6.7 | 7.0 | 7.2 | 10.0 |
| 53 | 3.7 | 3.7 | 3.7 | 3.7 | 3.7 | 3.7 | 3.7 | 3.7 | 3.7 | 3.7 | 3.7 | 3.7 | 3.7 | 3.7 | 3.7 | 3.7 | 3.7 | 3.7 | 3.7 | 3.7 |
| 54 | 3.7 | 3.7 | 3.7 | 3.7 | 3.7 | 3.7 | 3.7 | 3.7 | 3.7 | 3.7 | 3.7 | 3.7 | 4.5 | 5.3 | 3.7 | 3.7 | 3.7 | 7.4 | 7.8 | 3.7 |
| 55 | 3.7 | 3.7 | 4.2 | 4.3 | 4.9 | 5.1 | 5.4 | 6.3 | 8.1 | 9.8 | 12.1 | 13.2 | 15.0 | 16.3 | 17.8 | 19.4 | 20.8 | 21.3 | 22.3 | 23.0 |
| 56 | 3.7 | 4.2 | 5.3 | 6.2 | 7.4 | 8.0 | 8.9 | 10.5 | 11.9 | 13.3 | 14.4 | 15.7 | 15.1 | 15.9 | 16.8 | 17.7 | 18.7 | 20.4 | 21.3 | 22.2 |
| 57 | 3.7 | 4.3 | 5.6 | 6.7 | 8.5 | 9.9 | 11.4 | 12.6 | 13.2 | 14.0 | 14.9 | 16.2 | 16.5 | 16.9 | 17.2 | 17.6 | 18.0 | 19.4 | 20.1 | 22.0 |
| 58 | 3.9 | 4.6 | 5.7 | 6.7 | 8.2 | 9.5 | 11.0 | 12.3 | 12.8 | 13.8 | 15.0 | 16.4 | 16.7 | 17.3 | 18.0 | 18.7 | 19.4 | 20.6 | 21.4 | 23.1 |
| 59 | 3.7 | 3.9 | 4.9 | 5.8 | 7.1 | 8.2 | 9.5 | 10.7 | 11.3 | 12.4 | 13.4 | 14.6 | 14.8 | 15.4 | 16.1 | 16.8 | 17.4 | 18.3 | 18.9 | 20.6 |
| 60 | 3.7 | 4.2 | 5.2 | 6.2 | 7.5 | 8.6 | 9.9 | 11.0 | 11.4 | 12.4 | 13.4 | 14.6 | 14.7 | 15.4 | 16.0 | 16.6 | 17.3 | 18.3 | 19.0 | 20.5 |
| 61 | 3.9 | 4.6 | 5.7 | 6.7 | 8.1 | 9.2 | 10.6 | 11.7 | 12.1 | 13.0 | 14.0 | 15.2 | 15.5 | 16.2 | 16.9 | 17.5 | 18.2 | 19.3 | 20.0 | 21.5 |
| 62 | 3.7 | 3.7 | 3.9 | 4.5 | 5.4 | 6.2 | 7.0 | 7.7 | 8.0 | 8.6 | 9.3 | 10.1 | 10.2 | 10.7 | 11.1 | 11.5 | 12.0 | 12.5 | 12.9 | 13.9 |
| 63 | 3.7 | 3.7 | 4.5 | 5.3 | 6.2 | 7.0 | 8.0 | 8.7 | 9.0 | 9.6 | 10.3 | 11.3 | 11.5 | 12.0 | 12.5 | 13.0 | 13.5 | 14.3 | 14.7 | 15.7 |
| 64 | 3.7 | 3.7 | 3.7 | 3.7 | 3.7 | 3.7 | 3.7 | 3.7 | 3.7 | 3.7 | 3.7 | 3.7 | 3.7 | 3.7 | 3.7 | 3.7 | 3.7 | 3.7 | 3.7 | 3.7 |
| 65 | 3.7 | 3.7 | 4.4 | 5.1 | 6.0 | 6.8 | 7.7 | 8.3 | 8.6 | 9.2 | 9.8 | 10.7 | 11.0 | 11.4 | 11.9 | 12.3 | 12.7 | 13.4 | 13.8 | 14.8 |
| 66 | 3.7 | 3.9 | 4.9 | 5.9 | 6.8 | 7.7 | 8.7 | 9.3 | 9.7 | 10.3 | 11.0 | 12.0 | 12.4 | 12.9 | 13.4 | 13.9 | 14.4 | 15.3 | 15.8 | 16.9 |

Table A11: Nusselt number values in the laryngeal tracheal airway “LT” at flow rates ranging between 1 and 20 liters/minute

REFERENCES

1. WHO. Tobacco. Updated 26 July 2021. <https://www.who.int/news-room/fact-sheets/detail/tobacco>
2. Pankow JF. A consideration of the role of gas/particle partitioning in the deposition of nicotine and other tobacco smoke compounds in the respiratory tract. *Chemical research in toxicology*. Nov 2001;14(11):1465-81. doi:10.1021/tx0100901
3. Rodgman A, Perfetti T. *The Chemical Components of Tobacco and Tobacco Smoke, Second Edition*. 2013.
4. Stratton K, Shetty P, Wallace R, Bondurant S. Clearing the smoke: the science base for tobacco harm reduction—executive summary. *Tobacco control*. 2001;10(2):189. doi:10.1136/tc.10.2.189
5. R EC, K JB, Battey-Muse CM, Gardenhire DS. 2021 Year in Review: E-Cigarettes, Hookah Use, and Vaping Lung Injuries During the COVID-19 Pandemic. *Respir Care*. Jun 2022;67(6):709-714. doi:10.4187/respcare.09919
6. Zhu S-H, Sun JY, Bonnevie E, et al. Four hundred and sixty brands of e-cigarettes and counting: implications for product regulation. *Tobacco Control*. 2014;23(suppl 3):iii3-iii9. doi:10.1136/tobaccocontrol-2014-051670
7. Baassiri M, Talih S, Salman R, et al. Clouds and “throat hit”: Effects of liquid composition on nicotine emissions and physical characteristics of electronic cigarette aerosols. *Aerosol Science and Technology*. 2017/11/02 2017;51(11):1231-1239. doi:10.1080/02786826.2017.1341040
8. Cox S, Leigh NJ, Vanderbush TS, Choo E, Goniewicz ML, Dawkins L. An exploration into "do-it-yourself" (DIY) e-liquid mixing: Users' motivations, practices and product laboratory analysis. *Addict Behav Rep*. Jun 2019;9:100151. doi:10.1016/j.abrep.2018.100151
9. Kong G, Morean ME, Cavallo DA, Camenga DR, Krishnan-Sarin S. Reasons for Electronic Cigarette Experimentation and Discontinuation Among Adolescents and Young Adults. *Nicotine & Tobacco Research*. 2015;17(7):847-854. doi:10.1093/ntr/ntu257
10. Talih S, Salman R, Karaoghlanian N, et al. "Juice Monsters": Sub-Ohm Vaping and Toxic Volatile Aldehyde Emissions. *Chemical research in toxicology*. Oct 16 2017;30(10):1791-1793. doi:10.1021/acs.chemrestox.7b00212
11. El-Hellani A, Salman R, El-Hage R, et al. Nicotine and Carbonyl Emissions From Popular Electronic Cigarette Products: Correlation to Liquid Composition and Design Characteristics. *Nicotine & Tobacco Research*. 2018;20(2):215-223. doi:10.1093/ntr/ntw280
12. Haddad C, Salman R, El-Hellani A, Talih S, Shihadeh A, Saliba NA. Reactive Oxygen Species Emissions from Supra- and Sub-Ohm Electronic Cigarettes. *J Anal Toxicol*. Jan 1 2019;43(1):45-50. doi:10.1093/jat/bky065
13. United States Public Health Service Office of the Surgeon G, National Center for Chronic Disease P, Health Promotion Office on S, Health. Publications and Reports of the Surgeon General. *Smoking Cessation: A Report of the Surgeon General*. US Department of Health and Human Services; 2020.
14. Benowitz NL, Henningfield JE. Establishing a nicotine threshold for addiction. The implications for tobacco regulation. *N Engl J Med*. Jul 14 1994;331(2):123-5. doi:10.1056/nejm199407143310212

15. Henningfield JE, Benowitz NL, Slade J, Houston TP, Davis RM, Deitchman SD. Reducing the addictiveness of cigarettes. Council on Scientific Affairs, American Medical Association. *Tobacco control*. Autumn 1998;7(3):281-93. doi:10.1136/tc.7.3.281
16. Henningfield JE, Stapleton JM, Benowitz NL, Grayson RF, London ED. Higher levels of nicotine in arterial than in venous blood after cigarette smoking. *Drug and alcohol dependence*. Jun 1993;33(1):23-9. doi:10.1016/0376-8716(93)90030-t
17. Wayne GF, Connolly GN, Henningfield JE, Farone WA. Tobacco industry research and efforts to manipulate smoke particle size: implications for product regulation. *Nicotine & tobacco research : official journal of the Society for Research on Nicotine and Tobacco*. Apr 2008;10(4):613-25. doi:10.1080/14622200801978698
18. El Hourani M, Shihadeh A, Talih S, Eissenberg T. Comparison of nicotine emissions rate, 'nicotine flux', from heated, electronic and combustible tobacco products: data, trends and recommendations for regulation. *Tob Control*. Jan 27 2022;doi:10.1136/tobaccocontrol-2021-056850
19. Fabian LA, Canlas LL, Potts J, Pickworth WB. Ad lib smoking of Black & Mild cigarillos and cigarettes. *Nicotine & tobacco research : official journal of the Society for Research on Nicotine and Tobacco*. Mar 2012;14(3):368-71. doi:10.1093/ntr/ntr131
20. Yerger VB, McCandless PM. Menthol sensory qualities and smoking topography: a review of tobacco industry documents. *Tobacco control*. May 2011;20 Suppl 2(Suppl_2):ii37-43. doi:10.1136/tc.2010.041988
21. Alpert HR, Agaku IT, Connolly GN. A study of pyrazines in cigarettes and how additives might be used to enhance tobacco addiction. *Tobacco control*. Jul 2016;25(4):444-50. doi:10.1136/tobaccocontrol-2014-051943
22. Pankow JF. A Consideration of the Role of Gas/Particle Partitioning in the Deposition of Nicotine and Other Tobacco Smoke Compounds in the Respiratory Tract. *Chemical research in toxicology*. 2001/11/01 2001;14(11):1465-1481. doi:10.1021/tx0100901
23. Ingebrethsen BJ, Lyman CS, Gordin HH. Evaporative Deposition as a Mechanism of Sensory Stimulation, Memo, internal document of R. J. Reynolds Tobacco Company, April 22, 1991, 27 pp, Bates nos. 508297971/7997.
24. LOR LC, L. PH OF SMOKE, A REVIEW REPORT NUMBER: N-170. Lorillard Records; Master Settlement Agreement. <https://www.industrydocuments.ucsf.edu/docs/gghj0015>. 1976;
25. Creighton DE. The Significance of pH in Tobacco and Tobacco Smoke. <https://www.industrydocuments.ucsf.edu/docs/tslj0045>. 1987;
26. CE T. Implications and activities arising from correlation of smoke PH with nicotine impact, Other Smoke PH With Nicotine Impact, Other Smoke Qualities, And Cigarette sales. *RJ Reynolds Records; Minnesota Documents; Master Settlement Agreement*. 1973;
27. Maxwell JC. *The Scientific Papers of James Clerk Maxwell*. vol 2. Cambridge Library Collection - Physical Sciences. Cambridge University Press; 2011.
28. Hinds WC. *Aerosol Technology Properties, Behavior, and Measurement of Airborne Particles*. Second ed. John Wiley & Sons, INC.; 1999.
29. THEODORE L. BERGMAN ASL, FRANK P. INCROPERA, DAVID P. DEWITT. *Fundamentals of Heat and Mass Transfer* Seventh ed. JOHN WILEY & SONS; 2011.

30. Pankow JF, Kim K, Luo W, McWhirter KJ. Gas/Particle Partitioning Constants of Nicotine, Selected Toxicants, and Flavor Chemicals in Solutions of 50/50 Propylene Glycol/Glycerol As Used in Electronic Cigarettes. *Chemical research in toxicology*. Sep 17 2018;31(9):985-990. doi:10.1021/acs.chemrestox.8b00178
31. SCM. COSMO-RS. <https://www.scm.com/product/cosmo-rs/>
32. Lehtinen KEJ, Korhonen H, Dal Maso M. On the concept of condensation sink diameter. *Boreal Environment Research*. 12/10 2003;8:405-411.
33. Saleh R, Shihadeh A. Hygroscopic growth and evaporation in an aerosol with boundary heat and mass transfer. *Journal of Aerosol Science*. 2007/01/01/ 2007;38(1):1-16. doi:<https://doi.org/10.1016/j.jaerosci.2006.07.008>
34. Hiler M, Karaoghlanian N, Talih S, et al. Effects of electronic cigarette heating coil resistance and liquid nicotine concentration on user nicotine delivery, heart rate, subjective effects, puff topography, and liquid consumption. *Exp Clin Psychopharmacol*. Oct 2020;28(5):527-539. doi:10.1037/pha0000337
35. Eversole A, Budd S, Karaoghlanian N, Lipato T, Eissenberg T, Breland AB. Interactive effects of protonated nicotine concentration and device power on ENDS nicotine delivery, puff topography, and subjective effects. *Exp Clin Psychopharmacol*. Jun 13 2022;doi:10.1037/pha0000576
36. Maziak W, Taleb ZB, Bahelah R, et al. The global epidemiology of waterpipe smoking. *Tobacco control*. Mar 2015;24 Suppl 1:i3-i12. doi:10.1136/tobaccocontrol-2014-051903
37. Shihadeh A, Schubert J, Klaiany J, El Sabban M, Luch A, Saliba NA. Toxicant content, physical properties and biological activity of waterpipe tobacco smoke and its tobacco-free alternatives. *Tobacco control*. 2015;24(Suppl 1):i22. doi:10.1136/tobaccocontrol-2014-051907
38. El-Zaatari ZM, Chami HA, Zaatari GS. Health effects associated with waterpipe smoking. *Tobacco control*. 2015;24(Suppl 1):i31. doi:10.1136/tobaccocontrol-2014-051908
39. Maziak W. The waterpipe: time for action. *Addiction (Abingdon, England)*. Nov 2008;103(11):1763-7. doi:10.1111/j.1360-0443.2008.02327.x
40. Carroll MV, Chang J, Sidani JE, et al. Reigniting tobacco ritual: waterpipe tobacco smoking establishment culture in the United States. *Nicotine & tobacco research : official journal of the Society for Research on Nicotine and Tobacco*. Dec 2014;16(12):1549-58. doi:10.1093/ntr/ntu101
41. Salloum RG, Osman A, Maziak W, Thrasher JF. How popular is waterpipe tobacco smoking? Findings from internet search queries. *Tobacco control*. 2015;24(5):509-513. doi:10.1136/tobaccocontrol-2014-051675
42. Maziak W, Nakkash R, Bahelah R, Husseini A, Fanous N, Eissenberg T. Tobacco in the Arab world: old and new epidemics amidst policy paralysis. *Health policy and planning*. Sep 2014;29(6):784-94. doi:10.1093/heapol/czt055
43. Lipkus IM, Mays D. Comparing harm beliefs and risk perceptions among young adult waterpipe tobacco smokers and nonsmokers: Implications for cessation and prevention. *Addictive behaviors reports*. 2018;7:103-110. doi:10.1016/j.abrep.2018.03.003
44. Ozouni Davaji RB, Dadban Shahamat Y, Hajili Davaji F, et al. Patterns, Beliefs, Norms and Perceived Harms of Hookah Smoking in North Iran. *Asian Pacific journal of cancer prevention : APJCP*. 18(3):823-830. doi:10.22034/APJCP.2017.18.3.823

45. Hoffmann D, Hoffmann I, El-Bayoumy K. The less harmful cigarette: a controversial issue. a tribute to Ernst L. Wynder. *Chemical research in toxicology*. Jul 2001;14(7):767-90.
46. Shihadeh A, Saleh R. Polycyclic aromatic hydrocarbons, carbon monoxide, "tar", and nicotine in the mainstream smoke aerosol of the narghile water pipe. *Food and chemical toxicology : an international journal published for the British Industrial Biological Research Association*. May 2005;43(5):655-61. doi:10.1016/j.fct.2004.12.013
47. Shihadeh A, Azar S, Antonios C, Haddad A. Towards a topographical model of narghile water-pipe cafe smoking: a pilot study in a high socioeconomic status neighborhood of Beirut, Lebanon. *Pharmacology, biochemistry, and behavior*. Sep 2004;79(1):75-82. doi:10.1016/j.pbb.2004.06.005
48. Shihadeh A, Salman R, Jaroudi E, et al. Does switching to a tobacco-free waterpipe product reduce toxicant intake? A crossover study comparing CO, NO, PAH, volatile aldehydes, "tar" and nicotine yields. *Food and chemical toxicology : an international journal published for the British Industrial Biological Research Association*. May 2012;50(5):1494-8. doi:10.1016/j.fct.2012.02.041
49. Saleh R, Shihadeh A. Elevated toxicant yields with narghile waterpipes smoked using a plastic hose. *Food and chemical toxicology : an international journal published for the British Industrial Biological Research Association*. May 2008;46(5):1461-6. doi:10.1016/j.fct.2007.12.007
50. Siegmund B, Leitner E, Pfannhauser W. Development of a simple sample preparation technique for gas chromatographic-mass spectrometric determination of nicotine in edible nightshades (Solanaceae). *Journal of chromatography A*. Apr 30 1999;840(2):249-60.
51. Jawad M, Eissenberg T, Salman R, et al. Toxicant inhalation among singleton waterpipe tobacco users in natural settings. *Tobacco control*. May 28 2018;doi:10.1136/tobaccocontrol-2017-054230
52. Friedlander SK. *Smoke, Dust, and Haze Fundamentals of Aerosol Dynamics*. Second ed. Oxford University Press; 2000.
53. Monn C, Kindler P, Meile A, Brändli O. Ultrafine particle emissions from waterpipes. *Tobacco control*. 2007;16(6):390-393. doi:10.1136/tc.2007.021097
54. El Hourani M, Talih S, Salman R, et al. Comparison of CO, PAH, Nicotine, and Aldehyde Emissions in Waterpipe Tobacco Smoke Generated Using Electrical and Charcoal Heating Methods. *Chemical research in toxicology*. Jun 17 2019;32(6):1235-1240. doi:10.1021/acs.chemrestox.9b00045
55. Hammal F, Chappell A, Wild TC, et al. 'Herbal' but potentially hazardous: an analysis of the constituents and smoke emissions of tobacco-free waterpipe products and the air quality in the cafes where they are served. *Tobacco control*. May 2015;24(3):290-7. doi:10.1136/tobaccocontrol-2013-051169
56. Sepetdjian E, Shihadeh A, Saliba NA. Measurement of 16 polycyclic aromatic hydrocarbons in narghile waterpipe tobacco smoke. *Food and chemical toxicology : an international journal published for the British Industrial Biological Research Association*. May 2008;46(5):1582-90. doi:10.1016/j.fct.2007.12.028information
57. Hoffmann D, Djordjevic MV, Hoffmann I. The changing cigarette. *Preventive medicine*. Jul-Aug 1997;26(4):427-34. doi:10.1006/pmed.1997.0183
58. National Center for Biotechnology Information. PubChem Database. Pentanal, CID=8063 <https://pubchem.ncbi.nlm.nih.gov/compound/Pentanal>

59. Agaku IT, Filippidis FT, Vardavas CI, et al. Poly-tobacco use among adults in 44 countries during 2008-2012: evidence for an integrative and comprehensive approach in tobacco control. *Drug and alcohol dependence*. Jun 1 2014;139:60-70. doi:10.1016/j.drugalcdep.2014.03.003
60. Abdullah P, Costanian C, Khanlou N, Tamim H. Prevalence and characteristics of water-pipe smoking in Canada: results from the Canadian Tobacco Use Monitoring Survey. *Public health*. Jul 2017;148:102-108. doi:10.1016/j.puhe.2017.03.007
61. Hair E, Rath JM, Pitzer L, et al. Trajectories of Hookah Use: Harm Perceptions from Youth to Young Adulthood. *American Journal of Health Behavior*. 2017;41(3):240-247. doi:10.5993/AJHB.41.3.3
62. Cornacchione J, Wagoner KG, Wiseman KD, et al. Adolescent and Young Adult Perceptions of Hookah and Little Cigars/Cigarillos: Implications for Risk Messages. *Journal of health communication*. Jul 2016;21(7):818-25. doi:10.1080/10810730.2016.1177141
63. Monzer B, Sepetdjian E, Saliba N, Shihadeh A. Charcoal emissions as a source of CO and carcinogenic PAH in mainstream narghile waterpipe smoke. *Food and chemical toxicology : an international journal published for the British Industrial Biological Research Association*. Sep 2008;46(9):2991-5. doi:10.1016/j.fct.2008.05.031
64. Markowicz P, Löndahl J, Wierzbicka A, Suleiman R, Shihadeh A, Larsson L. A study on particles and some microbial markers in waterpipe tobacco smoke. *The Science of the total environment*. Nov 15 2014;499:107-13. doi:10.1016/j.scitotenv.2014.08.055
65. Shihadeh A, Eissenberg T, Rammah M, Salman R, Jaroudi E, El-Sabban M. Comparison of tobacco-containing and tobacco-free waterpipe products: effects on human alveolar cells. *Nicotine & tobacco research : official journal of the Society for Research on Nicotine and Tobacco*. Apr 2014;16(4):496-9. doi:10.1093/ntr/ntt193
66. Schubert J, Heinke V, Bewersdorff J, Luch A, Schulz TG. Waterpipe smoking: the role of humectants in the release of toxic carbonyls. *Archives of toxicology*. Aug 2012;86(8):1309-16. doi:10.1007/s00204-012-0884-5
67. Schubert J, Hahn J, Dettbarn G, Seidel A, Luch A, Schulz TG. Mainstream smoke of the waterpipe: does this environmental matrix reveal as significant source of toxic compounds? *Toxicology letters*. Sep 10 2011;205(3):279-84. doi:10.1016/j.toxlet.2011.06.017
68. Jacob P, 3rd, Abu Raddaha AH, Dempsey D, et al. Comparison of nicotine and carcinogen exposure with water pipe and cigarette smoking. *Cancer epidemiology, biomarkers & prevention : a publication of the American Association for Cancer Research, cosponsored by the American Society of Preventive Oncology*. May 2013;22(5):765-72. doi:10.1158/1055-9965.epi-12-1422
69. Shihadeh AL, Eissenberg TE. Significance of smoking machine toxicant yields to blood-level exposure in water pipe tobacco smokers. *Cancer epidemiology, biomarkers & prevention : a publication of the American Association for Cancer Research, cosponsored by the American Society of Preventive Oncology*. Nov 2011;20(11):2457-60. doi:10.1158/1055-9965.Epi-11-0586
70. Shafagoj YA, Mohammed FI, Hadidi KA. Hubble-bubble (water pipe) smoking: levels of nicotine and cotinine in plasma, saliva and urine. *International journal of clinical pharmacology and therapeutics*. Jun 2002;40(6):249-55.

71. Rastam S, Ward KD, Eissenberg T, Maziak W. Estimating the beginning of the waterpipe epidemic in Syria. *BMC Public Health*. 2004/08/04 2004;4(1):32. doi:10.1186/1471-2458-4-32
72. Martinasek MP, McDermott RJ, Martini L. Waterpipe (hookah) tobacco smoking among youth. *Current problems in pediatric and adolescent health care*. Feb 2011;41(2):34-57. doi:10.1016/j.cppeds.2010.10.001
73. Shihadeh A. Investigation of mainstream smoke aerosol of the argileh water pipe. *Food and chemical toxicology : an international journal published for the British Industrial Biological Research Association*. Jan 2003;41(1):143-52.
74. Brinkman MC, Kim H, Buehler SS, Adetona AM, Gordon SM, Clark PI. Evidence of compensation among waterpipe smokers using harm reduction components. *Tobacco control*. 2018;doi:10.1136/tobaccocontrol-2018-054502
75. Amazon.com. Hleeduo® Electronic Shisha Charcoal. Accessed 10/22, 2018. <https://www.amazon.com/Ren-Headstream-RY0811-Hleeduo%C2%AE-Electronic/dp/B005TQC6S4>
76. Amazon.com. New Generation Hookah Shisha Smokepan. Accessed 10/22, 2018. https://www.amazon.com/Generation-Hookah-Smokepan-Electronic-Ceramic/product-reviews/B00ANXRSWW/ref=cm_cr_arp_d_viewpnt_lft?filterByStar=positive&pageNumber=1
77. Talih S, Balhas Z, Eissenberg T, et al. Effects of user puff topography, device voltage, and liquid nicotine concentration on electronic cigarette nicotine yield: measurements and model predictions. *Nicotine & tobacco research : official journal of the Society for Research on Nicotine and Tobacco*. Feb 2015;17(2):150-7. doi:10.1093/ntr/ntu174
78. Saliba NA, El Hellani A, Honein E, et al. Surface chemistry of electronic cigarette electrical heating coils: Effects of metal type on propylene glycol thermal decomposition. *Journal of Analytical and Applied Pyrolysis*. 2018/09/01/ 2018;134:520-525. doi:<https://doi.org/10.1016/j.jaap.2018.07.019>
79. Uchiyama S, Tomizawa T, Inaba Y, Kunugita N. Simultaneous determination of volatile organic compounds and carbonyls in mainstream cigarette smoke using a sorbent cartridge followed by two-step elution. *Journal of chromatography A*. Nov 1 2013;1314:31-7. doi:10.1016/j.chroma.2013.09.019
80. Al Rashidi M, Shihadeh A, Saliba NA. Volatile aldehydes in the mainstream smoke of the narghile waterpipe. *Food and chemical toxicology : an international journal published for the British Industrial Biological Research Association*. Nov 2008;46(11):3546-9. doi:10.1016/j.fct.2008.09.007
81. Fowles J, Dybing E. Application of toxicological risk assessment principles to the chemical constituents of cigarette smoke. *Tobacco control*. Dec 2003;12(4):424-30.
82. Saliba N, El Hellani A, Honein E, et al. *Surface Chemistry of Electronic Cigarette Electrical Heating Coils: Effects of Metal Type on Propylene Glycol Thermal Decomposition*. 2018.
83. Talih S, Balhas Z, Salman R, Karaoghlanian N, Shihadeh A. "Direct Dripping": A High-Temperature, High-Formaldehyde Emission Electronic Cigarette Use Method. *Nicotine & tobacco research : official journal of the Society for Research on Nicotine and Tobacco*. Apr 2016;18(4):453-9. doi:10.1093/ntr/ntv080
84. Kosmider L, Sobczak A, Fik M, et al. Carbonyl compounds in electronic cigarette vapors: effects of nicotine solvent and battery output voltage. *Nicotine &*

tobacco research : official journal of the Society for Research on Nicotine and Tobacco.
Oct 2014;16(10):1319-26. doi:10.1093/ntr/ntu078

85. WHO. Tobacco. <https://www.who.int/news-room/fact-sheets/detail/tobacco>

86. Carter LP, Stitzer ML, Henningfield JE, O'Connor RJ, Cummings KM, Hatsukami DK. Abuse liability assessment of tobacco products including potential reduced exposure products. *Cancer epidemiology, biomarkers & prevention : a publication of the American Association for Cancer Research, cosponsored by the American Society of Preventive Oncology.* Dec 2009;18(12):3241-62. doi:10.1158/1055-9965.Epi-09-0948

87. Allain F, Minogianis EA, Roberts DC, Samaha AN. How fast and how often: The pharmacokinetics of drug use are decisive in addiction. *Neuroscience and biobehavioral reviews.* Sep 2015;56:166-79. doi:10.1016/j.neubiorev.2015.06.012

88. Djordjevic MV, Stellman SD, Zang E. Doses of Nicotine and Lung Carcinogens Delivered to Cigarette Smokers. *JNCI: Journal of the National Cancer Institute.* 2000;92(2):106-111. doi:10.1093/jnci/92.2.106

89. Shihadeh A, Eissenberg T. Electronic cigarette effectiveness and abuse liability: predicting and regulating nicotine flux. *Nicotine & tobacco research : official journal of the Society for Research on Nicotine and Tobacco.* 2015;17(2):158-162. doi:10.1093/ntr/ntu175

90. Samara F, Alam IA, ElSayed Y. Midwakh: Assessment of levels of Carcinogenic Polycyclic Aromatic Hydrocarbons (PAHs) and Nicotine in Dokha Tobacco Smoke. *J Anal Toxicol.* Jan 21 2021;doi:10.1093/jat/bkab012

91. Prochaska JJ, Vogel EA, Benowitz N. Nicotine delivery and cigarette equivalents from vaping a JUULpod. *Tobacco control.* Mar 24 2021;doi:10.1136/tobaccocontrol-2020-056367

92. Eissenberg T, Soule E, Shihadeh A. 'Open-System' electronic cigarettes cannot be regulated effectively. *Tobacco control.* Mar 2021;30(2):234-235. doi:10.1136/tobaccocontrol-2019-055499

93. Armitage AK, Alexander J, Hopkins R, Ward C. Evaluation of a low to middle tar/medium nicotine cigarette designed to maintain nicotine delivery to the smoker. *Psychopharmacology.* 1988/12/01 1988;96(4):447-453. doi:10.1007/BF02180022

94. Hammond D, Fong GT, Cummings KM, O'Connor RJ, Giovino GA, McNeill A. Cigarette yields and human exposure: a comparison of alternative testing regimens. *Cancer epidemiology, biomarkers & prevention : a publication of the American Association for Cancer Research, cosponsored by the American Society of Preventive Oncology.* Aug 2006;15(8):1495-501. doi:10.1158/1055-9965.Epi-06-0047

95. Melikian A, Djordjevic M, Hosey J, et al. Gender Differences Relative to Smoking Behavior and Emissions of Toxins From Mainstream Cigarette Smoke. *Nicotine & tobacco research : official journal of the Society for Research on Nicotine and Tobacco.* 04/01 2007;9:377-87. doi:10.1080/14622200701188836

96. Watson CV, Richter P, de Castro BR, et al. Smoking Behavior and Exposure: Results of a Menthol Cigarette Cross-over Study. *American journal of health behavior.* 2017;41(3):309-319. doi:10.5993/AJHB.41.3.10

97. Pauwels CGGM, Boots AW, Visser WF, et al. Characteristic Human Individual Puffing Profiles Can Generate More TNCO than ISO and Health Canada Regimes on Smoking Machine When the Same Brand Is Smoked. *Int J Environ Res Public Health.* 2020;17(9):3225. doi:10.3390/ijerph17093225

98. Gee J, Prasad K, Slayford S, et al. Assessment of tobacco heating product THP1.0. Part 8: Study to determine puffing topography, mouth level exposure and consumption among Japanese users. *Regulatory Toxicology and Pharmacology*. 2018/03/01/ 2018;93:84-91. doi:<https://doi.org/10.1016/j.yrtph.2017.08.005>
99. Jones J, Slayford S, Gray A, Brick K, Prasad K, Proctor C. A cross-category puffing topography, mouth level exposure and consumption study among Italian users of tobacco and nicotine products. *Scientific Reports*. 2020/01/08 2020;10(1):12. doi:10.1038/s41598-019-55410-5
100. Piadé JJ, Roemer E, Dempsey R, et al. Toxicological assessment of kretek cigarettes: Part 2: Kretek and American-blended cigarettes, smoke chemistry and in vitro toxicity. *Regulatory Toxicology and Pharmacology*. 2014/12/15/ 2014;70:S15-S25. doi:<https://doi.org/10.1016/j.yrtph.2014.12.001>
101. Goel R, Trushin N, Reilly SM, et al. A Survey of Nicotine Yields in Small Cigar Smoke: Influence of Cigar Design and Smoking Regimens. *Nicotine & tobacco research : official journal of the Society for Research on Nicotine and Tobacco*. Sep 4 2018;20(10):1250-1257. doi:10.1093/ntr/ntx220
102. Laugesen M, Fowles J. Marlboro UltraSmooth: a potentially reduced exposure cigarette? *Tobacco control*. 2006;15(6):430-435. doi:10.1136/tc.2006.016055
103. Farsalinos KE, Yannovits N, Sarri T, Voudris V, Poulas K. Nicotine Delivery to the Aerosol of a Heat-Not-Burn Tobacco Product: Comparison With a Tobacco Cigarette and E-Cigarettes. *Nicotine & tobacco research : official journal of the Society for Research on Nicotine and Tobacco*. Jul 9 2018;20(8):1004-1009. doi:10.1093/ntr/ntx138
104. Carmines E, Gillman I. Comparison of the Yield of Very Low Nicotine Content Cigarettes to the Top 100 United States Brand Styles. *Beiträge zur Tabakforschung International/Contributions to Tobacco Research*. 08/01 2019;28:253-266. doi:10.2478/cttr-2019-0005
105. Rickert WS, Robinson JC, Bray DF, Rogers B, Collishaw NE. Characterization of tobacco products: A comparative study of the tar, nicotine, and carbon monoxide yields of cigars, manufactured cigarettes, and cigarettes made from fine-cut tobacco. Article. *Preventive Medicine*. 1985;14(2):226-233. doi:10.1016/0091-7435(85)90038-6
106. Marcilla A, Beltran MI, Gómez-Siurana A, Berenguer D, Martínez-Castellanos I. Comparison between the mainstream smoke of eleven RYO tobacco brands and the reference tobacco 3R4F. *Toxicol Rep*. 2014;1:122-136. doi:10.1016/j.toxrep.2014.05.004
107. Darrall KG, Figgins JA. Roll-your-own smoke yields: theoretical and practical aspects. *Tobacco control*. Summer 1998;7(2):168-75. doi:10.1136/tc.7.2.168
108. McAdam K, Davis P, Ashmore L, et al. Influence of machine-based puffing parameters on aerosol and smoke emissions from next generation nicotine inhalation products. *Regul Toxicol Pharmacol*. Feb 2019;101:156-165. doi:10.1016/j.yrtph.2018.11.006
109. Forster M, Fiebelkorn S, Yurteri C, et al. Assessment of novel tobacco heating product THP1.0. Part 3: Comprehensive chemical characterisation of harmful and potentially harmful aerosol emissions. *Regul Toxicol Pharmacol*. Mar 2018;93:14-33. doi:10.1016/j.yrtph.2017.10.006
110. Kosmider L, Sobczak A, Szołtysek-Bołdys I, et al. Assessment of nicotine concentration in electronic nicotine delivery system (ENDS) liquids and precision of dosing to aerosol. *Przegląd lekarski*. 2015;72(10):500-4.

111. Behar RZ, Hua M, Talbot P. Puffing topography and nicotine intake of electronic cigarette users. *PLoS One*. 2015;10(2):e0117222. doi:10.1371/journal.pone.0117222
112. Farsalinos K, Poulas K, Voudris V. Changes in Puffing Topography and Nicotine Consumption Depending on the Power Setting of Electronic Cigarettes. *Nicotine & Tobacco Research*. 2018;20(8):993-997. doi:10.1093/ntr/ntx219
113. St Helen G, Shahid M, Chu S, Benowitz NL. Impact of e-liquid flavors on e-cigarette vaping behavior. *Drug and alcohol dependence*. Aug 1 2018;189:42-48. doi:10.1016/j.drugalcdep.2018.04.032
114. Talih S, Salman R, El-Hage R, et al. A comparison of the electrical characteristics, liquid composition, and toxicant emissions of JUUL USA and JUUL UK e-cigarettes. *Sci Rep*. Apr 30 2020;10(1):7322. doi:10.1038/s41598-020-64414-5
115. Talih S, Salman R, El-Hage R, et al. Characteristics and toxicant emissions of JUUL electronic cigarettes. *Tobacco control*. 2019;28(6):678. doi:10.1136/tobaccocontrol-2018-054616
116. Reilly SM, Bitzer ZT, Goel R, Trushin N, Richie JP. Free Radical, Carbonyl, and Nicotine Levels Produced by Juul Electronic Cigarettes. *Nicotine & tobacco research : official journal of the Society for Research on Nicotine and Tobacco*. Aug 19 2019;21(9):1274-1278. doi:10.1093/ntr/nty221
117. Soha Talih RS, Eric Soule, Racehl El Hage, Ebrahim Karam, Nareg Karaoghlanian, Ahmad El-Hellani, Najat Saliba, Alan Shihadeh. Electrical features, liquid composition and toxicant emissions from ‘pod-mod’-like disposable electronic cigarettes (Under Review). 2021.
118. Ramôa CP, Shihadeh A, Salman R, Eissenberg T. Group Waterpipe Tobacco Smoking Increases Smoke Toxicant Concentration. *Nicotine & tobacco research : official journal of the Society for Research on Nicotine and Tobacco*. May 2016;18(5):770-6. doi:10.1093/ntr/ntv271
119. Katurji M, Daher N, Sheheitli H, Saleh R, Shihadeh A. Direct measurement of toxicants inhaled by water pipe users in the natural environment using a real-time in situ sampling technique. *Inhalation toxicology*. Nov 2010;22(13):1101-9. doi:10.3109/08958378.2010.524265
120. Pickworth WB, Rosenberry ZR, Yi D, Pitts EN, Lord-Adem W, Koszowski B. Cigarillo and Little Cigar Mainstream Smoke Constituents from Replicated Human Smoking. *Chemical research in toxicology*. Apr 16 2018;31(4):251-258. doi:10.1021/acs.chemrestox.7b00312
121. Irwin S, Klaus DB, Dietrich H, Alan C. On the Chemistry of Cigar Smoke: Comparisons between Experimental Little and Large Cigars. *Beiträge zur Tabakforschung International/Contributions to Tobacco Research*. 1976;8(6):367-377. doi:<https://doi.org/10.2478/cttr-2013-0405>
122. Watson CH, Polzin GM, Calafat AM, Ashley DL. Determination of tar, nicotine, and carbon monoxide yields in the smoke of bidi cigarettes. *Nicotine & Tobacco Research*. 2003;5(5):747-753. doi:10.1080/1462220031000158591
123. Pakhale SS, Maru GB. Distribution of major and minor alkaloids in tobacco, mainstream and sidestream smoke of popular Indian smoking products. *Food and chemical toxicology : an international journal published for the British Industrial Biological Research Association*. Dec 1998;36(12):1131-8. doi:10.1016/s0278-6915(98)00071-4

124. Ltd OP. NiQuitin Pre-Quit Clear 21mg Patch. <https://www.medicines.org.uk/emc/product/2938/smpc>
125. Shiffman S, Scholl SM, Mao J, et al. Using Nicotine Gum to Assist Nondaily Smokers in Quitting: A Randomized Clinical Trial. *Nicotine & Tobacco Research*. 2019;doi:10.1093/ntr/ntz090
126. Lande RG. What is the role of nicotine gum in the treatment of nicotine addiction? <https://www.medscape.com/answers/287555-158527/what-is-the-role-of-nicotine-gum-in-the-treatment-of-nicotine-addiction>
127. Talih S, Balhas Z, Salman R, et al. Transport phenomena governing nicotine emissions from electronic cigarettes: model formulation and experimental investigation. *Aerosol Sci Technol*. 2017;51(1):1-11. doi:10.1080/02786826.2016.1257853
128. Cooper M, Harrell MB, Perry CL. A Qualitative Approach to Understanding Real-World Electronic Cigarette Use: Implications for Measurement and Regulation. *Prev Chronic Dis*. Jan 14 2016;13:E07. doi:10.5888/pcd13.150502
129. Baweja R, Curci KM, Yingst J, et al. Views of Experienced Electronic Cigarette Users. *Addict Res Theory*. 2016;24(1):80-88. doi:10.3109/16066359.2015.1077947
130. Do EK, O'Connor K, Perks SN, et al. E-cigarette device and liquid characteristics and E-cigarette dependence: A pilot study of pod-based and disposable E-cigarette users. *Addict Behav*. Jan 2022;124:107117. doi:10.1016/j.addbeh.2021.107117